Journal of Natural Gas Science and Engineering 29 (2016) 530–549

Contents lists available at ScienceDirect

Journal of Natural Gas Science and Engineering

journal homepage: www.elsevier.com/locate/jngse

Invited review

Modeling of uniform CO_2 corrosion of mild steel in gas transportation systems: A review

Aria Kahyarian*, Marc Singer, Srdjan Nesic

Institute for Corrosion and Multiphase Flow Technology, Ohio University, Athens, OH, USA

ARTICLE INFO

Article history:
Received 31 July 2015
Received in revised form
30 December 2015
Accepted 31 December 2015
Available online 6 January 2016

Keywords:
Carbon dioxide
Mild steel
Corrosion
Uniform
Modeling

ABSTRACT

The state of the art with regards the mechanistic understanding of uniform carbon dioxide corrosion of mild steel is reviewed and the corresponding mathematical models are presented. The existing predictive models are categorized into three groups, termed: empirical/semi-empirical, elementary mechanistic, and comprehensive mechanistic. With emphasis on mechanistic models, selected key publications are reviewed and the limits and advantages of each group of models are discussed. Furthermore, the ability of the existing models to be extended and account for more complex corrosion scenarios is discussed.

Contents

1. Introduction 531
2. Review of the fundamentals 531
 2.1. Water chemistry in CO_2 corrosion 531
 2.2. Electrochemical reactions in CO_2 corrosion 532
  2.2.1. Cathodic reactions 533
  2.2.2. Anodic reactions 535
  2.2.3. Charge transfer rate calculations 536
 2.3. Mass transfer in corroding systems 537
3. The mathematical models of CO_2 corrosion 538
 3.1. Empirical/semi-empirical models 538
 3.2. Elementary mechanistic models 538
 3.3. Comprehensive mechanistic models 539
4. Extension beyond basic calculations 540
 4.1. Additional corrosive species 540
 4.2. Effect of corrosion product layer 541
 4.3. Top of the line corrosion 543
5. Conclusions 545
 Acknowledgment 545
 Nomenclature 546
 References 546

* Corresponding author.
E-mail address: ak702711@ohio.edu (A. Kahyarian).

http://dx.doi.org/10.1016/j.jngse.2015.12.052
1875-5100/

1. Introduction

Reliable estimation of corrosion rate is one of the key considerations for design of transmission pipelines and related infrastructure for natural gas production and processing. Predicted corrosion rates directly affect major design decisions, such as material selection, pipe wall thickness allowance, pipe diameter and hence velocity, etc. as well as operational planning such as need for corrosion mitigation, inspection and monitoring. Underestimation of corrosion rates may therefore lead to failure, with health, safety and environmental hazards as well as significant financial losses due to production interruption, equipment replacement, etc. On the other hand, gross overestimation can have a strong impact on the economic aspects of a project.

In natural gas extraction, carbon dioxide (CO_2) is almost always present as a byproduct, and in its hydrated form (H_2CO_3), it is a well-known corrosive species. Mild steel uniform corrosion rate estimations associated with CO_2 in wet natural gas systems has historically been done by "worst case" empirical/semi-empirical models developed in the 1980s and 1990s (de Waard et al., 1991; Dugstad et al., 1994; Olsen et al., 2005). Whilst these models have been extensively used, primarily due to their simplicity, their application is limited by the narrow range of conditions they cover. On the other hand, increasing interest for exploration and gas production in harsher, more corrosive environments pushes the applications of these models beyond the point where they can be confidently used. Even though improving the models to address the ever more challenging industrial demands has been slow, advancements in the mechanistic understanding of the underlying processes in CO_2 corrosion has provided new opportunities for development of more robust mechanistic models, with the ability to perform well beyond the scope covered by the previous empirical/semi-empirical models. Having strong roots in the physicochemical theory underlying the corrosion process, the mechanistic models introduced over the past two decades have provided the flexibility required to cover various conditions and include new processes in corrosion rate calculations.

Uniform CO_2 corrosion of mild steel can be considered as one of the most studied and well understood corrosion systems. In addition to numerous studies covering specific aspects of this corrosion system, several holistic reviews of the underlying physicochemical processes (Nešić and Sun, 2010; Nešić, 2011, 2007; Revie, 2011; Richardson, 2009) as well as reviews of uniform corrosion rate prediction models (Kapusta et al., 2004; Nešić et al., 1997; Nyborg, 2006, 2002; Olsen, 2003) are available in the literature.

The present review is primarily focused on progress in development of mechanistic mathematical models of aqueous CO_2 corrosion of mild steel and describes the state of the art. In this context, the fundamental physicochemical processes underlying uniform CO_2 corrosion are discussed and the corresponding mathematical relationships are presented. The mechanistic aspects of the chemical and electrochemical reactions, as well as mass transfer processes are covered in some detail.

The mathematical models developed to date are here categorized into three main groups: (*i*) empirical/semi-empirical, (*ii*) elementary mechanistic, and (*iii*) comprehensive mechanistic models. As the focus is on the mechanistic models, the empirical and semi-empirical models are only briefly discussed as background/historical information. In the discussion of the mechanistic models, selected key studies are reviewed and the strength and limitations of the various modeling approaches are presented. Furthermore, the ability of the various types of models to be adapted to more complex conditions and be extended to include additional phenomena such as those seen in the presence of additional corrosive species (*e.g.* H_2S, organic acids, etc.), corrosion product layer formation, and top of the line corrosion (TLC) is discussed.

Table 1
Homogeneous chemical reactions in water/CO_2 environment.

Reaction	Equilibrium equation
$CO_{2_{(g)}} \leftrightharpoons CO_{2_{(aq)}}$	$H_{CO_2} = \frac{\left[CO_{2_{(aq)}}\right]}{pCO_{2_{(g)}}}$ (1)
$CO_{2(aq)} + H_2O_{(l)} \leftrightharpoons H_2CO_{3(aq)}$	$K_{hyd} = \frac{k_{f,hyd}}{k_{b,hyd}} = \frac{[H_2CO_3]}{\left[CO_{2_{(aq)}}\right]}$ (2)
$H_2CO_{3(aq)} \leftrightharpoons HCO^-_{3(aq)} + H^+_{(aq)}$	$K_{ca} = \frac{k_{f,ca}}{k_{b,ca}} = \frac{\left[HCO_3^-\right][H^+]}{[H_2CO_3]}$ (3)
$HCO^-_{3(aq)} \leftrightharpoons CO^{2-}_{3(aq)} + H^+_{(aq)}$	$K_{bi} = \frac{k_{f,bi}}{k_{b,bi}} = \frac{\left[CO_3^{2-}\right][H^+]}{\left[HCO_3^-\right]}$ (4)
$H_2O_{(l)} \leftrightharpoons OH^-_{(aq)} + H^+_{(aq)}$	$K_w = \frac{k_{f,w}}{k_{b,w}} = \left[OH^-\right]\left[H^+\right]$ (5)

2. Review of the fundamentals

2.1. Water chemistry in CO_2 corrosion

A comprehensive knowledge of the water composition is essential for accurate calculations of corrosion rates. Chemical equilibria relating to dissolved CO_2 and its carbonate derivatives in the bulk solution has been extensively studied (Butler, 1991; Stumm and Morgan, 1995; Zeebe and Wolf-Gladrow, 2001). However, reaction kinetics relating to these equilibria, particularly at the interface between the bulk fluid and the metal surface have only been accounted for in the more recent mechanistic studies (Nordsveen et al., 2003; Pots, 1995; Remita et al., 2008; Turgoose et al., 1992).

The main chemical reactions in CO_2 aqueous solutions, their corresponding chemical equilibria, and kinetic rate constants are presented in Table 1 and Table 2. The water speciation in the bulk solution can be readily calculated by simultaneous solution of equilibrium expressions for all species along with the electroneutrality constraint (Nešić and Sun, 2010). An example of the results of such calculations for an open system with constant partial pressure of 1 bar CO_2 at various pH values is shown in Fig. 1. The effect of reaction kinetics on surface concentrations needs to be accounted for differently, as discussed in detail in section 2.3. It should be noted that here it was assumed that the infinite dilution theory is valid, *i.e.* the activity coefficients for all the chemical species are assumed to be unity. This assumption is consistent with the literature considered in the present review. While it provides a reasonable estimation of speciation for majority of aqueous CO_2 systems seen in gas transportation applications, it also greatly simplifies the resulting mathematical expressions. The effect of non-ideal behavior seen at high pressures and concentrations is discussed elsewhere: for water chemistry (Duan and Li, 2008; Duan and Sun, 2003; Duan et al., 2006; Li and Duan, 2007; Mohamed et al., 2011), and for the mass transfer (Fosbøl et al., 2009; Newman and Thomas-Alyea, 2004). It is important to note that the modifications required to cover this non-ideal behavior can be

Table 2
Equilibrium and reaction rate constants for chemical reactions shown in Table 1.

Constant	Units	Reference
$H_{CO_2} = \frac{1}{1.00258}\exp\left(93.4517\left(\frac{100}{T}\right) - 60.2409 + 23.3585\ln\left(\frac{T}{100}\right) + \left(0.023517 - 0.023656\left(\frac{T}{100}\right) + 0.0047036\left(\frac{T}{100}\right)^2\right)S‰\right)$	M.bar^{-1}	(Dickson and Goyet, 1994; Weiss, 1974; Zeebe and Wolf-Gladrow, 2001)
$K_w = \exp\left(\frac{-13847.26}{T} + 148.9652 - 23.6521\ln T + \left(\frac{118.67}{T} - 5.977 + 1.0495\ln T\right)S‰^{0.5} + 0.01615\,S‰\right)$	M^2	(Dickson and Goyet, 1994; Millero, 1995; Zeebe and Wolf-Gladrow, 2001)
$k_{b,w} = 7.8 \times 10^{10}$	M^{-1} s^{-1}	(Delahay, 1952)
$K_{hyd} = 2.85 \times 10^{-3}$	–	(Palmer and Eldik, 1983)
$k_{f,hyd} = 10^{\left(329.85 - 110.541\times\log T - \frac{17265.4}{T}\right)}$	s^{-1}	(Palmer and Eldik, 1983)
$K_{ca} = 378.6\exp\left(\frac{-2307.1266}{T} + 2.83655 - 1.5529413\ln T + \left(\frac{-4.0484}{T} - 0.20760841\right)S‰^{0.5} + 0.08468345\,S‰ - 0.00654208\,S‰^{1.5} + \ln(1 - 0.001005\,S‰)\right)$	M	(Dickson and Goyet, 1994; Roy et al., 1993; Zeebe and Wolf-Gladrow, 2001)
$k_{f,ca} = 10^{(5.71 + 0.0526\times T_C - 2.94\times10^{-4}\times T_C^2 + 7.91\times10^{-7}\times T_C^3)}$	s^{-1}	(Green, 1972)
$K_{bi} = \exp\left(\frac{-3351.6106}{T} - 9.226508 - 0.2005743\ln T + \left(\frac{-23.9722}{T} - 0.1069017773\right)S‰^{0.5} + 0.1130822\,S‰ - 0.00846934\,S‰^{1.5} + \ln(1 - 0.001005\,S‰)\right)$	M	(Dickson and Goyet, 1994; Roy et al., 1993; Zeebe and Wolf-Gladrow, 2001)
$k_{f,bi} = 10^9$	s^{-1}	(Nordsveen et al., 2003)[a]

[a] The value of $k_{f,bi}$ is estimated and it is not based on experimental measurements.

readily included into the general framework of the mechanistic models discussed in the following chapters.

2.2. Electrochemical reactions in CO_2 corrosion

The cathodic and the anodic reactions on the metal surface are what define the corrosion process as a heterogeneous phenomenon. Despite long-term research focused on the electrochemical reactions involved in CO_2 corrosion, the predictive models rely on best assumptions about the exact reaction mechanisms.

Table 3 summarizes the key electrochemical reactions associated with the species commonly considered electroactive in aqueous CO_2 corrosion of mild steel. Each reaction shown is an overall reaction and usually consists of a few elementary steps which are discussed in the following sections. Reaction 1 to Reaction 4 are the possible cathodic reactions in a CO_2 containing aqueous environment. Reaction 1 and Reaction 2 are the well-known hydrogen evolution reactions from hydrogen ion and water, common for all aqueous acidic systems. Reaction 3 is the so called "direct" reduction of carbonic acid (H_2CO_3), which has been identified by numerous authors as the main contribution of CO_2 to the enhancement of corrosion rate, when compared to strong acids (de Waard and Milliams, 1975a; Gray et al., 1989; Nešić et al., 1996a; Nordsveen et al., 2003). Similarly, Reaction 4 is the reduction of bicarbonate ion which is believed to be significant at near-neutral and alkaline pH values due to high bicarbonate ion concentration, as depicted in Fig. 1 (Gray et al., 1990; Han et al., 2011c; Ogundele and White, 1987, 1986). In the literature, both the reduction of carbonic acid and bicarbonate ion are known as "direct reduction" mechanism, meaning that the undissociated acid is adsorbed and directly reduced at the metal surface during the corrosion process, to evolve hydrogen. An alternative mechanism known as "buffering effect" is also proposed in the literature. This mechanism suggests that the dissociation of the carbonic acid in the vicinity of the metal/solution interface replenishes the hydrogen ion concentration at the metal surface as it is consumed by the corrosion process (Remita et al., 2008; Tran et al., 2015). It should be noted that the "direct reduction" mechanism allows for the possibility for carbonic acid (or any other weak acid) to also act as a buffer (Nešić et al., 2001; Nordsveen et al., 2003; Pots, 1995), while this is not considered to be the dominant effect. On the other hand, the "buffering effect"

Fig. 1. Concentration of different species in CO_2/water equilibrium at various pH values, $pCO_2 = 1$ bar, T = 298 K, and 0.5 M NaCl in an open system with a constant CO_2 partial pressure.

Table 3
Possible electrochemical reactions in CO_2 corrosion of mild steel.

Reaction number	Electrochemical reaction	Dominant reaction type
Reaction 1	$H^+_{(aq)} + e^- \leftrightharpoons \frac{1}{2}H_{2(g)}$	Cathodic
Reaction 2	$H_2O_{(l)} + e^- \leftrightharpoons OH^-_{(aq)} + \frac{1}{2}\ H_{2(g)}$	Cathodic
Reaction 3	$H_2CO_{3(aq)} + e^- \leftrightharpoons HCO^-_{3(aq)} + \frac{1}{2}\ H_{2(g)}$	Cathodic
Reaction 4	$HCO^-_{3(aq)} + e^- \leftrightharpoons CO^{2-}_{3(aq)} + \frac{1}{2}H_{2(g)}$	Cathodic
Reaction 5	$Fe^{2+}_{(aq)} + 2e^- \leftrightharpoons Fe_{(s)}$	Anodic

mechanism excludes the possibility of "direct reduction" of weak acids. Therefore the divergence of the two mechanisms, "buffering effect" and "direct reduction", is in the assumed electro-activity of the undissociated weak acid.

Similar mechanistic arguments are frequent in corrosion studies. For example, the direct reduction of water is common knowledge; it has been recently proven that another weak acid – hydrogen sulfide is also directly reduced (Kittel et al., 2013; Zheng et al., 2014). However, the arguments on the reduction mechanism of carbonic as well as organic acids are still unsettled, although now it appears that "direct reduction" mechanism is not significant (Amri et al., 2011; Hurlen et al., 1984; Remita et al., 2008; Tran et al., 2015, 2013).

2.2.1. Cathodic reactions

The exact mechanism of cathodic reactions in the presence of weak acids in general, and carbonic acid in particular, remains open to debate. The major controversy is related to the role of undissociated carbonic acid. This protracted controversy remains unsolved due to the intrinsic complexity of the system, especially as the weak acids are at equilibrium with the hydrogen ion at all times, making it hard to distinguish the two. In aqueous solutions, based on the definition of reversible potential, it can be shown that weak acids such as carbonic acid and bicarbonate ion, are thermodynamically identical (Gray et al., 1989). Furthermore, the fast kinetics of coupled homogeneous chemical reactions (see Table 2), makes it difficult to deploy the majority of standard electroanalytical techniques in order to resolve this issue. Therefore, the main method used to study this system was through the quantitative analysis of charge transfer rates.

In the last four decades, the mechanistic understanding of CO_2 corrosion and the development of more inclusive mathematical descriptions of this system has been undergoing concurrent evolution. De Waard and Milliams were amongst the first researchers attempting to elucidate the mechanism of CO_2 corrosion (de Waard and Milliams, 1975a, 1975b). Based on a quantitative analysis, De Waard and Milliams proposed a mechanism for CO_2 corrosion where the dominant cathodic reaction is the "direct reduction" of the undissociated carbonic acid. This mechanism was further supported by Wieckowski et al. based on their studies with cyclic voltammetry (Więckowski et al., 1983a).

In 1977, Schmitt and Rothmann (Schmitt and Rothmann, 1977) proposed a mechanism for the cathodic reaction in aqueous CO_2 environments based on their study of the limiting current response to flow velocity and partial pressure of CO_2. Schmitt and Rothman reported that the limiting current consists of both flow dependent and flow independent components. It was shown that the flow dependent part of the limiting current was governed by transfer of hydrogen ion and undissociated carbonic acid, while the flow independent part was suggested to be limited by the slow reaction rate of adsorbed CO_2 to give carbonic acid, in the so called hydration step. The relevance of the adsorption in hydration of CO_2 was later challenged by Wieckowski et al. in their radiotracer study of the iron/CO_2 system (Więckowski et al., 1983b).

The mechanism of cathodic reactions in CO_2 environment was further discussed by Gray et al. (Gray et al., 1990, 1989) by introducing a mathematical model for CO_2 corrosion of mild steel. Using the proposed mechanism of Schmitt and Rothmann as the basis of their model while considering the radiotracer study of Wieckowski et al. (1983b), Gray et al. suggested that the adsorption step of CO_2 introduced by Schmitt and Rothmann (1977) was unnecessary to explain the limiting currents observed in CO_2 environments. This model is based on concurrent reduction of hydrogen ions and carbonic acid, while the effect of slow hydration of carbonic acid in the bulk solution was also included. This mechanism has become the most commonly accepted mechanism of CO_2 corrosion ever since.

In more recent studies, a few attempts have been made in order to quantitatively describe the increased corrosion rates in CO_2 systems solely through the buffering effect of carbonic acid on hydrogen ion concentration. Remita et al. (2008) reported a quantitative analysis of cathodic currents in CO_2 saturated solutions. The authors claimed that they could predict the cathodic currents without considering direct reduction of carbonic acid. Their model is based on the reaction rate constant of the hydrogen ion reduction obtained from experimental data in deaerated acidic solutions and the homogeneous reactions related to CO_2 equilibria. Based on the good agreement between the predicted voltammograms and the experimental data, the authors concluded that the direct carbonic acid reduction reaction is not necessary to quantitatively explain the higher cathodic current densities observed in CO_2 systems.

Considering the limited experimental scope of Remita et al. study (only pH4 and 1 bar CO_2), their conclusion about the insignificant contribution of carbonic acid reduction to the cathodic current may not be readily extrapolated to conditions where carbonic acid concentration is many orders of magnitude higher than the hydrogen ion concentration (see Fig. 1 at pH 6 as an example). Additionally, Remita et al. compared the surface pH measurements in unbuffered acidic solution with solutions buffered with carbonic acid. The lower surface pH values obtained in carbonic acid environment was considered as additional proof for the buffering effect mechanism. However, this decreasing trend of surface pH would be expected for both mechanisms. Therefore, surface pH measurements are not able to provide conclusive arguments on the mechanism of cathodic reaction.

In a more experimentally extensive approach, Tran et al. (2015) aimed to distinguish between the direct reduction and buffering effect mechanism by studying the sensitivity of the pure charge transfer controlled cathodic currents to the concentration of undissociated acid, a similar approach as that previously used for acetic acid (Hurlen et al., 1984; Tran et al., 2013). This is depicted in Fig. 2 by comparison of the hypothetical voltammograms of these two reaction mechanisms. Fig. 2A represents the direct reduction mechanism where the net cathodic current is the summation of the current from both hydrogen ion and the undissociated weak acid (H_2CO_3) reduction. Fig. 2B shows the expected behavior of the buffering effect mechanism where the cathodic currents are only defined by hydrogen ion reduction and the weak acid is only an additional source of hydrogen ions. Here both mechanisms show

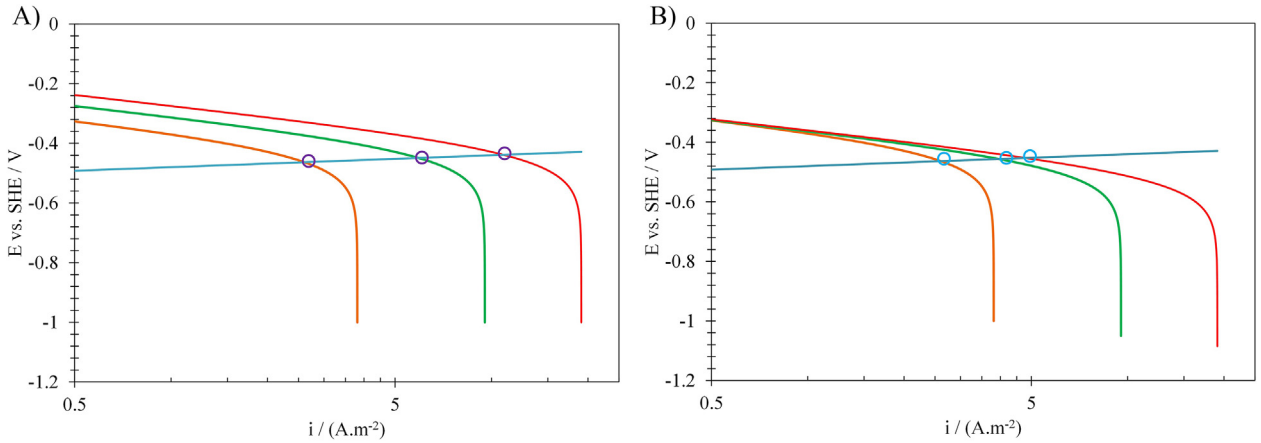

Fig. 2. An illustration of hypothetical polarization curves expected at a constant pH; cathodic lines for three concentrations of a weak acid (red > green > orange). Blue line represents the anodic reaction. A) direct reduction mechanism (de Waard and Milliams, 1975a, 1975b) B) buffering effect mechanism. (Tran et al., 2013).[1]

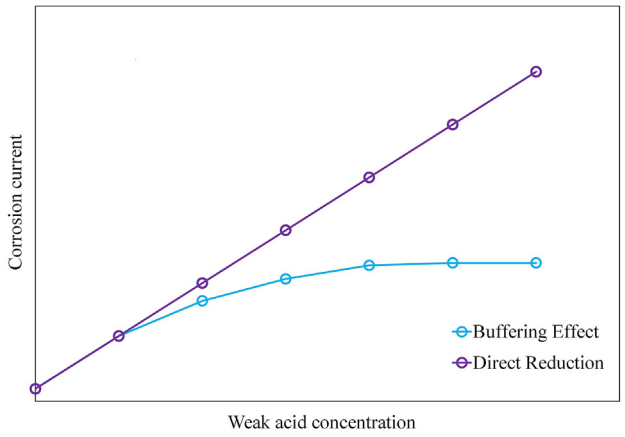

Fig. 3. Illustration of the corrosion current/rate behavior for the different cathodic reaction mechanisms shown in Fig. 2 (Tran et al., 2013).[1]

identical limiting current behavior with increasing concentration of the weak acid. For the case of carbonic acid, this behavior can be explained by considering that the limiting current is the superposition of mass transfer limiting current of hydrogen ions and chemical reaction limiting current of CO_2 hydration as the rate determining steps. Therefore, the associated faster electrochemical reactions, whether in form of direct reduction of carbonic acid, or via the buffering effect mechanism, cannot be distinguished in the potential range governed by the limiting currents.

However, at charge transfer controlled current conditions (at higher potentials), a distinctive behavior is expected. In direct reduction mechanism (Fig. 2A), both hydrogen ions and carbonic acid are reactive, therefore, at a constant pH the net current increases by rising concentrations of the weak acid. At similar conditions, in the buffering effect mechanism, when the undissociated weak acid is not reduced (Fig. 2B), the charge transfer controlled current remains unchanged. Therefore these two mechanisms can be distinguished by studying the behavior of the charge transfer controlled currents at various weak acid concentrations (carbonic acid in this case).

The significance of this mechanistic discussion in corrosion rate predictive models is illustrated in Fig. 3. This graph shows that predicted corrosion rates at higher partial pressures of CO_2 (high concentrations of carbonic acid) can be vastly different, depending on the adopted mechanism in the model. If carbonic acid is not considered as an electro-active species (as in buffering effect mechanism), a maximum charge transfer controlled corrosion current will be reached at some high partial pressure of CO_2. If it is adopted that carbonic acid is directly reduced, the predicted corrosion current would be steadily increasing with increasing CO_2 partial pressure.

The main difficulty in testing such a hypothesis in CO_2 environments is the lack of ability to observe the pure charge transfer cathodic current on mild steel at typical experimental conditions, due to the interference by the anodic iron dissolution reaction. Therefore, Tran et al. suggested using stainless steel, being a more noble metal, where the interference by the anodic reaction is negligible for a wide range of cathodic potentials. The polarization data reported in their work clearly show a Tafel behavior (pure charge transfer controlled current), which appears not to respond to the change in partial pressure of CO_2, up to 10 bar. This observation is in agreement with the behavior expected in the buffering effect mechanism (see Fig. 2B). However, the author's suggestion that the same cathodic reaction mechanism detected on stainless steel is valid for mild steel as well, needs to be further investigated, as the effect of alloying compounds (~20 wt. % Cr, and 10 wt. % Ni) and their corresponding oxide films on the electro-activity of the metal surface could be significant. As discussed in the following chapter, the sensitivity of the hydrogen evolution reactions to the state of the metal surface is well known, which suggests that this assumption may not be acceptable without proof.

2.2.1.1. Hydrogen evolution reaction. The hydrogen evolution reaction is one of the most widely studied electrochemical reactions. Volmer, Heyrovsky, and Tafel steps (Reaction 6, Reaction 7, and Reaction 8, respectively) are the most commonly accepted steps in the hydrogen evolution mechanism (Bockris and Reddy, 1973; Conway and Tilak, 2002), while alternative mechanisms such as the one involving molecular hydrogen ion (H_2^+) is also proposed (Juodkazis et al., 2014, 2011). A wealth of information is available in the literature on the mechanistic behavior and kinetic parameters for hydrogen evolution reaction, based on experimental results (Bockris and Koch, 1961; Brug et al., 1984; Sheng et al., 2010; Stern, 1955), as well as theoretical analyses (Bockris and Potter, 1952;

[1] Reproduced with permission from NACE International, Houston, TX. All rights reserved. T. Tran, B. Bruce, S. Nešic, B Tribollet, Investigation of the electrochemical mechanisms for acetic acid corrosion of mild steel, Corrosion, 70, 3, 2013. ©NACE International 1945.

Table 4
Kinetic parameters of hydrogen ion reduction on iron.

Reference	Electrolyte	b [mV]	m vs. pH
(Bockris et al., 1962)	1 N [SO_4^{2-}], 0.5 N [Fe^{2+}], pH: 2.0–4.0	116 ± 7	−1
(Bockris and Koch, 1961)	0.5 N HCl	133 ± 4	NA
(McCafferty and Hackerman, 1972)	1 N [Cl^-], [H^+]: 0.2–2.96	120 ± 10	−1
(Hurlen, 1960)	1 N [Cl^-], 0.1 < pH < 3	117	−1
(Chin and Nobe, 1972)	1 N [Cl^-], 0.0 < pH < 1.8	115	−1
(Felloni, 1968)	1 N [Cl^-], 0.07 < pH < 2.92	123–155	−0.5
	1 N [SO_4^{2-}], 0.30 < pH < 3.74	120–190	−0.5
(Stern, 1955)	4 wt. % NaCl, 1.42 < pH < 5.26	100	−0.5

Conway and Salomon, 1964; Gennero de Chialvo and Chialvo, 2001, 2000, 1999, 1998; Tavares et al., 2001; Tilak and Chen, 1993). A quick review of the literature readily indicates the complex nature of this reaction, where a significant change in the kinetics may occur with variation of the electrode material (Bockris and Koch, 1961; Bockris et al., 1957; Schuldiner, 1961; Thomas and Nobe, 1970), surface preparation and crystal structure (Bockris et al., 1957; Brug et al., 1984), pH (Schuldiner, 1954a; Sheng et al., 2010), overpotential (Schuldiner, 1961, 1954b), adsorbed species, and trace impurities (Bockris et al., 1965, 1957; Qian et al., 1999, 1998). This suggests that seeking universal kinetic mechanism and parameters for the hydrogen evolution reactions is neither reasonable nor possible.

$$H^+ + e^- \rightleftharpoons H_{ad} \quad Volmer\ acidic\ HER \qquad \text{Reaction 6}$$

$$H_{ad} + H^+ + e^- \rightleftharpoons H_2 \quad Heyrovsky\ acidic\ HER \qquad \text{Reaction 7}$$

$$H_{ad} + H_{ad} \rightleftharpoons H_2 \quad Tafel \qquad \text{Reaction 8}$$

For the case of hydrogen ion reduction on iron, it is commonly considered that the reduction reaction occurs with the Volmer reaction being the rate determining step (Kittel et al., 2013; Nešić et al., 1996b; Remita et al., 2008; Tran et al., 2013; Tribollet et al., 2014; Zheng et al., 2014), generally based on the findings of Bockris et al. (Bockris and Koch, 1961; Bockris et al., 1965; Delahay, 1970; Pentland et al., 1957). This mechanism has a theoretical value of 0.5 for the transfer coefficient (Tafel slope of $b = 118$ mV at 25 °C), and reaction order of $m = -1$ with respect to pH (Conway and Salomon, 1964). These parameters have been to some extent experimentally verified, with some deviations from expected theoretical values also reported in the literature (see Table 4). As shown in Table 4 most studies cover very acidic solutions while in less acidic solutions, *i.e.* pH 3 and higher, the experimental verification of these parameters is limited by interference from the iron oxidation reaction.

For hydrogen evolution from water the similar elementary steps are suggested (Safizadeh et al., 2015). Assuming the Volmer step to be rate determining, Tafel slope of 118 mV and reaction order of −0.5 vs. pH is expected. The reported data in literature are generally in agreement with the expected reaction order of −0.5, while the reported Tafel slopes are significantly deviating from the theoretical value of 118 mV (Bockris et al., 1962; Gray et al., 1990, 1989; Hurlen, 1960; Stern, 1955).

The mechanism of hydrogen evolution from other weak acids can be described by an analogy with that of the hydrogen ion reduction described above. Using a general formulation the elementary steps of hydrogen evolution reaction are shown below by Reaction 9 to Reaction 11, where HA denotes any weak acid such as water, carbonic acid, acetic acid, hydrogen sulfide, etc. (Amri et al., 2011; Mishra et al., 1997; Ogundele and White, 1987; Tran et al., 2013; Więckowski et al., 1983b). The rate determining step in the weak acid reduction mechanisms is rarely discussed in the literature, *e.g.* (Ogundele and White, 1987). However, the commonly used expressions for exchange current density (Han et al., 2011c; Nešić et al., 1996a; Nordsveen et al., 2003; Zheng et al., 2014) need to assume the Volmer step being rate determining, in order to be consistent with theory.

$$HA + e^- \rightleftharpoons H_{ad} + A^- \quad Volmer \qquad \text{Reaction 9}$$

$$H_{ad} + HA + e^- \rightleftharpoons H_2 + A^- \quad Heyrovsky \qquad \text{Reaction 10}$$

$$H_{ad} + H_{ad} \rightleftharpoons H_2 \quad Tafel \qquad \text{Reaction 11}$$

2.2.2. Anodic reactions

The most accepted mechanism for iron dissolution in acidic media, which is the main anodic reaction in mild steel corrosion, has been proposed by Bockris et al. (1961) (BDD mechanism) as shown by Reaction 12 to Reaction 14. In the original study the authors compared the theoretically calculated parameters from a series of possible mechanisms with their own experimentally obtained values. For their proposed mechanism, the measured Tafel slope of 40 mV agreed well with the theoretical value. The experimentally determined reaction order vs. pH of 0.9 ± 0.05 was close to the theoretical value of 1. The reaction order of ferrous ion concentration of 0.8, obtained experimentally, was also close to the theoretical value of 0.75. The authors also noted that the reaction order versus pH decreases from 1 to β/2 at pH values above 4, where β is the transfer coefficient of Reaction 13 (Bockris et al., 1961). However, in other studies a rather broad variation of these parameters has been measured (see Table 5) indicating the possibility of alternative mechanisms.

$$Fe + OH^- \rightleftharpoons Fe[OH]_{ads} + e^- \qquad \text{Reaction 12}$$

$$Fe[OH]_{ads} \rightleftharpoons Fe[OH]^+ + e^- \qquad \text{Reaction 13}$$

$$Fe[OH]^+ \rightleftharpoons Fe^{2+} + OH^- \qquad \text{Reaction 14}$$

Table 5 summarizes some of the reported kinetic parameters for iron dissolution in acidic solutions.

Nevertheless, the BDD mechanism has been directly used in the mathematical models of CO_2 corrosion for many years (de Waard and Milliams, 1975a; Gray et al., 1990; Nešić et al., 1996a), while dissolved CO_2 and its associated carbonic species were shown to directly affect the anodic dissolution reaction (Davies and Burstein, 1980; Nešić et al., 1996b; Videm, 1993). Davis and Burstein (1980) proposed an analogous reaction mechanism to the BDD mechanism by including the effect of bicarbonate ion on iron dissolution. They suggest that bicarbonate ion can act as an intermediate in the iron dissolution process in a similar way as hydroxide ion does in

Table 5
Kinetic parameters of iron dissolution in acidic media.

Reference Fe	Electrolyte	b [mV]	m vs. pH	m vs. pFe
(Bockris et al., 1962)	1 N $[SO_4^{2-}]$, 0.5 N $[Fe^{2+}]$ pH: 1.2–4.9	40	0.9 ± 0.05	−0.8
(McCafferty and Hackerman, 1972)	1 N $[Cl^-]$, 0.2 < $[H^+]$ < 2.96	65–70	0.7	NA
(Hurlen, 1960)	1 N $[Cl^-]$, 0.1 < pH < 3	29	1	−2
(Chin and Nobe, 1972)	1 N $[Cl^-]$, 0.0 < pH < 1.8	70	0.6	NA
(Felloni, 1968)	1 N $[Cl^-]$, 0.07 < pH < 2.92	70–44	0.83–1.52	NA
	1 N $[SO_4^{2-}]$, 0.30 < pH < 3.74	32–25	1.52–1.43	

Table 6
Electrochemical parameters for exchange current density calculation based on Equation 10.[a]

Reaction	Exchange current density
Reaction 1	$i_{0,H} = i_{0,H,ref}\left(\frac{C^b_{H^+}}{C^b_{H^+,ref}}\right)^{(1-\alpha_H)} e^{\frac{-E_a}{R}\left(\frac{1}{T}-\frac{1}{T_{ref}}\right)}$
Reaction 2	$i_{0,H_2O} = i_{0,W,ref}\left(\frac{C^b_{H^+}}{C^b_{H^+,ref}}\right)^{-\alpha_W} e^{\frac{-E_a}{R}\left(\frac{1}{T}-\frac{1}{T_{ref}}\right)}$
Reaction 3	$i_{0,CA} = i_{0,CA,ref}\left(\frac{C^b_{H^+}}{C^b_{H^+,ref}}\right)^{-\alpha_{CA}}\left(\frac{C^b_{H_2CO_3}}{C^b_{H_2CO_3,ref}}\right)^{1} e^{\frac{-E_a}{R}\left(\frac{1}{T}-\frac{1}{T_{ref}}\right)}$
Reaction 4	$i_{0,BC} = i_{0,BC,ref}\left(\frac{C^b_{H^+}}{C^b_{H^+,ref}}\right)^{-(1+\alpha_{BC})}\left(\frac{C^b_{H_2CO_3}}{C^b_{H_2CO_3,ref}}\right)^{1} e^{\frac{-E_a}{R}\left(\frac{1}{T}-\frac{1}{T_{ref}}\right)}$
Reaction 5[b]	$i_{0,Fe} = i_{0,Fe,ref}\left(\frac{C^b_{H^+}}{10^{-4}}\right)^{a_1}\left(\frac{C^b_{CO_2}}{0.0366}\right)^{a_2} e^{\frac{-E_a}{R}\left(\frac{1}{T}-\frac{1}{298.15}\right)}$ $pH<4: a_1=-2,\ n\alpha_{a,Fe}=2$ $pH>5: a_1=0,\ n\alpha_{a,Fe}=0.5$ $PCO_2<1: a_2=1$ $PCO_2\geq 1: a_2=0$

[a] The values for activation energies, reference concentrations and exchange current densities of Reaction 1 to Reaction 3 is listed in (Nešić et al., 1996a) and for Reaction 4 in (Han et al., 2011c). Note that the exchange current density expressions presented here are based on Equation (10) and are not necessarily similar to those shown in the references provided.

[b] The expression of exchange current density of iron dissolution reaction is the semi-empirical expression from (Nešić et al., 1996b).

strong acid solutions. The direct involvement of bicarbonate ion on iron dissolution is also supported by other studies (*e.g.* (Ogundele and White, 1986)).

Nesic et al. (1996b) conducted a study of iron dissolution in CO_2 environments, illustrating the sensitivity of this reaction to pH and CO_2 partial pressure. Using potentiodynamic sweeps and galvanostatic measurements, Nesic et al. (1996b) suggested iron dissolution in CO_2 system has a generally different mechanism compared to the well-known BDD mechanism. In a similar fashion as Davis and Burstein (1980), Nesic et al. assumed that the effect of carbonic species on iron dissolution is through formation of a chemical ligand acting as a catalyst, involving CO_2 due to its high and constant concentration at all pH values. Reaction 15 to Reaction 20 show the proposed mechanism where CO_2 and its derivatives serve as intermediate species, in a similar role as hydroxide ion has in the BDD mechanism. Here the rate determining step changes from Reaction 19 at pH values below 4 to Reaction 17 at pH values of 5 and higher. Quantitatively, the authors suggest that the effect of CO_2 is proportional to surface coverage, so that when pCO_2<0.1 bar – the coverage is very small and the presence of dissolved CO_2 has an insignificant effect on the anodic dissolution rate, the effect then increases with increasing pCO_2 and at pCO_2 > 1 bar the metal surface coverage reaches saturation, and the effect vanishes. The mathematical expression corresponding to this mechanism is shown in Table 6.

$$Fe + CO_2 \rightleftharpoons FeCO_{2\ ads} \qquad \text{Reaction 15}$$

$$FeCO_{2\ ads} + H_2O \rightleftharpoons FeHCO_{3\ ads} + H^+ + e^- \qquad \text{Reaction 16}$$

$$FeHCO_{3\ ads} \rightleftharpoons FeHCO^+_{3\ ads} + e^- \qquad \text{Reaction 17}$$

$$FeHCO^+_{3\ ads} + H_2O \rightleftharpoons FeOH_2CO_{3\ ads} + H^+ \qquad \text{Reaction 18}$$

$$FeOH_2CO_{3\ ads} \rightleftharpoons FeOH_2CO_{3\ sol} \qquad \text{Reaction 19}$$

$$FeOH_2CO_{3\ sol} + 2H^+ \rightleftharpoons Fe^{2+} + CO_2 + 2\ H_2O \qquad \text{Reaction 20}$$

The abovementioned mechanisms proposed by Davis and Burstein (1980) and also Nesic et al. (1996b) are in conflict with the findings of Wiekowski et al. (1983b) where their radiotracer study in CO_2 saturated solution showed no detectable adsorption of labeled carbon on the metal surface. Additionally, in a more recent study by Almedia et al. (2015) it was shown that the electrochemical impedance spectrum of iron in hydrochloric acid and saturated CO_2 solution have identical characteristic loops, suggesting that the mechanism of iron dissolution is similar in both cases and does not include any significant adsorption of CO_2 and/or its derivatives.

2.2.3. Charge transfer rate calculations

For an elementary electrochemical reaction (Reaction 21) the rate, expressed in terms of current density, can be calculated using Equation (6) (Anderko, 2010; Bard and Faulkner, 2001).

$$O + e^- \rightleftharpoons R \qquad \text{Reaction 21}$$

$$i = -i_0\left[\frac{C^s_O}{C^b_O}e^{-\frac{\alpha F\eta}{RT}} - \frac{C^s_R}{C^b_R}e^{\frac{(1-\alpha)F\eta}{RT}}\right] \qquad (6)$$

where overpotential (η) and exchange current density (i_o) are defined as follows:

$$\eta = E - E_{rev} \qquad (7)$$

$$i_0 = nFK_0C_O^{b1-\alpha}C_R^{b\alpha} \qquad (8)$$

Considering a known exchange current density, i_0^{ref}, at reference conditions ($C^b_{O,ref}, C^b_{R,ref}, T_{ref}$), one can use an Arrhenius type equation for the standard reaction rate constant, $K_0 = k_0e^{-E_a/RT}$, where the pre-exponential parameter (k_0) can be obtained from Equation (8) as:

$$k_0 = \frac{i_0^{ref}}{nFC^b_{O,\ ref}{}^{1-\alpha}C^b_{R,\ ref}{}^{\alpha}e^{\frac{-E_a}{RT_{ref}}}} \qquad (9)$$

Using Equation (8) and Equation (9), as well as Arrhenius'

equation for standard reaction rate constant, the exchange current density at a different temperature and bulk concentration of species can be found via Equation (10).

$$i_0 = i_0^{ref}\left(\frac{C_O^b}{C_{O,ref}^b}\right)^{1-\alpha}\left(\frac{C_R^b}{C_{R,ref}^b}\right)^{\alpha} e^{\frac{-E_a}{R}\left(\frac{1}{T}-\frac{1}{T_{ref}}\right)} \tag{10}$$

At high values of overpotential and pure charge transfer control, Equation (6) is simplified to the so called Tafel approximation. For example, for cathodic current it is:

$$i = -i_0 10^{\frac{-\eta}{b}} \tag{11}$$

where Tafel slope (b) is defined as:

$$b = -\frac{RT}{\alpha nF}$$

Assuming the rate determining (slow) step being the Volmer step for all hydrogen evolution reactions discussed previously, the exchange current densities in both Equation (6) and Equation (11) could be calculated as shown in Table 6.

2.3. Mass transfer in corroding systems

Considering the heterogeneity of the corrosion process, mass transfer calculations are required to define the concentration of electroactive species at the reaction site which is the metal surface. It has been shown that neglecting the mass transfer limitation in CO_2 corrosion rate calculation leads to significant overestimation of the corrosion rate (de Waard et al., 1995; Nyborg et al., 2000).

In a general form, Equation (12) describes the current density of an electrochemical reaction based on the mass transfer of the reactant from the bulk solution, at steady state.

$$i = nFk_m\left(C^b - C^s\right) \tag{12}$$

where k_m is the mass transfer coefficient:

$$k_m = \frac{Sh\ D}{L} \tag{13}$$

and C^b and C^s are the concentrations of the reactant in the bulk solution and at the metal surface, respectively. The value of C^s in Equation (12) is generally unknown and defined by the kinetics of the charge transfer reaction. However, in pure mass transfer limiting conditions the surface concentration of the reactant approaches zero. Therefore, Equation (12) can be used to calculate the mass transfer limiting current density as described by Equation (14).

$$i_{lim} = nFk_mC^b \tag{14}$$

The mass transfer coefficient for variety of flow conditions has been the subject of numerous studies. For example, the mass transfer limiting current for a rotating disc electrode can be derived theoretically due to laminar flow conditions, and is known as the Levich equation. For a rotating cylinder electrode, the turbulent flow correlation of Eisenberg et al. (1954) is often used. The mass transfer correlation in fully developed turbulent flow through smooth, straight pipes was defined by Berger and Hau (1977), where the Sherwood number (Sh) is correlated to the Reynolds number (Re) and the Schmidt number (Sc), as in Equation (15).

$$Sh = 0.0165\ Re^{0.86}Sc^{0.33}$$
$$8\times10^3 < Re < 2\times10^5, 1000 < Sc < 6000 \tag{15}$$

For various other flow regimes and geometries such as multiphase flow, U-bends, elbows, etc., similar correlations exist in the literature (Coney and Board, 1981; Cussler, 1997; Poulson, 1991; Wang and Shirazi, 2001; Wang et al., 1998).

In case of mixed mass transfer and charge transfer control of the cathodic reaction rate, the effect of mass transfer on net current (i_{net}) of an elementary electron transfer reaction can be theoretically derived, as shown by Equation (16), where the i_{ct} is the charge transfer controlled current and i_{lim} is the mass transfer limiting current defined by Equation (14).

$$\frac{1}{i_{net}} = \frac{1}{i_{ct}} + \frac{1}{i_{lim}} \tag{16}$$

Equation (16) has been commonly used in elementary mechanistic models of CO_2 corrosion (Gray et al., 1990, 1989; Nešić et al., 1996a), as well as in semi-empirical models (de Waard et al., 1995). This approach only considers the mass transfer of an individual species based on molecular diffusion and convection, independently from other species in the solution. In a system with multiple electro-active species that are involved in chemical reactions with each other, Equation (14) to Equation (16) fail to properly describe the mass transfer process, as discussed in chapter 3.2. In that case, the mass transfer of the chemical species needs to be described by the so called Nernst–Planck equation. This is a mass conservation equation that accounts for the effect of molecular diffusion and convection as well as simultaneous interaction between different species via homogeneous chemical reactions and through forming of an electrical potential field (often referred to as electromigration, or simply migration). For an incompressible fluid and dilute solutions, the flux of species can be written as (Newman and Thomas-Alyea, 2004):

$$N_i = -z_iu_iFC_i\nabla\phi - D_i\nabla C_i + \nu C_i \tag{17}$$

The Nernst–Planck equation describing mass conservation of species i in the presence of homogenous chemical reactions (R_i) is then:

$$\frac{\partial C_i}{\partial t} = -\nabla\cdot N_i + R_i \tag{18}$$

Using the Einstein-Smoluchowski estimation for mobility of ions for one-dimensional calculations, Equation (17) and Equation (18) yield Equation (19) and Equation (20) respectively, which are the building blocks of any comprehensive mechanistic model of multicomponent mass transport in reacting ionic solutions (Newman and Thomas-Alyea, 2004).

$$N_i = -D_i\frac{\partial C_i}{\partial x} - \frac{z_iD_iFC_i}{RT}\frac{\partial\phi}{\partial x} + \nu_xC_i \tag{19}$$

$$\frac{\partial C_i}{\partial t} = -D_i\frac{\partial}{\partial x}\frac{\partial C_i}{\partial x} - \frac{\partial}{\partial x}\left(\frac{z_iD_iFC_i}{RT}\frac{\partial\phi}{\partial x}\right) + \nu_x\frac{\partial C_i}{\partial x} + R_i \tag{20}$$

Unlike in the simple version of the mass transfer model (Equation (14) to Equation (16)), using the Nernst–Planck equation requires knowledge of the velocity field in the fluid near the metal surface. For the case of rotating disc electrodes, an analytical solution for the velocity profile in the form of a power series is known (Newman and Thomas-Alyea, 2004). Neglecting the higher order terms of this power series, Equation (21) describes the velocity profile in the solution near the electrode where $a = 0.510$, and Equation (22) provides the diffusion layer thickness (Newman and

Thomas-Alyea, 2004).

$$v_x = -a\Omega\left(\frac{\Omega}{\upsilon}\right)^{1/2} x^2 \tag{21}$$

$$\delta = \left(\frac{3D_{lim}}{a\upsilon}\right)^{1/3}\left(\frac{\Omega}{\upsilon}\right)^{-1/2} \tag{22}$$

However, for practical applications such as flow in transmission gas pipelines, conditions are very different from the laminar flow case described above, primarily due to turbulent mixing. In turbulent flow, one has to rely on empirical expressions describing the level of mixing in the mass transfer boundary layer, usually through an eddy diffusivity profile (Aravinth, 2000; Davies, 1972).

3. The mathematical models of CO_2 corrosion

Mathematical models of CO_2 corrosion can be categorized into three main groups, based on how much they rely on theoretical foundations described above:

Empirical/semi-empirical models are based on fitting of preselected mathematical functions to experimentally obtained corrosion rate data. In purely empirical models these functions have no real meaning and are arbitrarily chosen, while with semi-empirical models these functions are at least partially rooted in the theoretical foundations of the corrosion phenomena. These types of models are strictly limited to the experimental conditions used in their calibration, with little or no extrapolation capability.

Elementary mechanistic models are also based on mathematical functions, but in this case they are rooted in physicochemical theory of the corrosion process. However, in order to maintain simplicity, these models resort to simplification and decoupling of the various processes, *e.g.* mass transfer, chemical reactions and charge transfer phenomena. These models can be used to extrapolate predictions outside the range of experimental data used in their development, as long as the governing physicochemical processes are valid.

Comprehensive mechanistic models are deeply rooted in fundamental physicochemical laws, such as the ones described above. The underlying charge transfer, chemical and mass transfer processes are described comprehensively and are coupled with each other. While these models are computationally and mathematically more demanding, they enable more accurate predictions, they are easier to extend by adding new physics and their extrapolation capability is superior.

3.1. Empirical/semi-empirical models

Generally, empirical/semi-empirical models are simple predictive tools developed when limited fundamental understanding is available. In some cases, the basic mathematical functions used in these models may originate from rudimentary approximations of the fundamental physicochemical processes underlying the corrosion phenomena, however, the more elaborate aspects are accounted for by introducing correction factors in the model (Nešić et al., 1997; Nyborg, 2002). In most cases these factors are best-fit functions based on limited experimental data with no theoretical significance. This lack of theoretical meaning makes any combination of these empirical correction factors (required to cover more complex conditions) – dubious, to say the least. More importantly, due to this general lack of theoretical underpinning, these models cannot be reliably extrapolated outside the conditions used for their development. For the same reason these models have very limited flexibility needed for further extensions to account for new data and require recalibration of the model with the entire dataset to accommodate any such extension. To date, many variations of empirical/semi-empirical models are found that address a particular application (de Waard and Lotz, 1993; de Waard and Milliams, 1975b; de Waard et al., 1995, 1991; Dugstad et al., 1994; Jangama and Srinivasan, 1997; Olsen et al., 2005; Pots et al., 2002).

In an attempt to focus this review on the more recent mechanistic developments in CO_2 corrosion modeling, the discussion of empirical/semi-empirical models is limited to a brief review of the work by de Waard et al. due to its significance in shaping the understanding of CO_2 corrosion as we know it today. However, numerous reviews on empirical and semi-empirical models are available in the literature for further reference (Kapusta et al., 2004; Nešić, 2007; Nešić et al., 1997; Nyborg, 2006, 2002; Nyborg et al., 2000; Olsen, 2003).

de Waard and Milliams based their original model on a linear pH dependence of the corrosion current obtained from equating a simple charge transfer rate expression of anodic and cathodic currents at the corrosion potential, shown as Equation (23).

$$\log i_{corr} = -A \quad pH + B \tag{23}$$

By correlating this equation with their experimental data, the constant A was obtained ($A = 1.3$). de Waard and Milliams then attempted to develop a mechanistic explanation of CO_2 corrosion by comparing the empirical value for A with the ones obtained based on a few different hypothetical mechanisms. Finally the following "catalytic" mechanism for the cathodic reaction was proposed.

$$H_2CO_{3_{(aq)}} + e^- \rightarrow HCO^-_{3(aq)} + \frac{1}{2}\, H_{2(g)} \qquad \text{Reaction 22}$$

$$HCO^-_{3(aq)} + H^+_{(aq)} \leftrightharpoons H_2CO_{3_{(aq)}} \qquad \text{Reaction 23}$$

This enabled them to derive a simple expression for the corrosion rate as a function of temperature and partial pressure of CO_2, which remained the most popular way to predict corrosion rates for decades, and is still in use today. However simplistic and questionable, this was a first attempt at modeling of CO_2 corrosion in a mechanistic way, using theoretical considerations. The important effects of pH, flow, and slow CO_2 hydration, on the cathodic reaction were not considered in this first attempt and were added later.

A number of new effects such as: pH, flow rate, non-ideal solutions, protective scales, glycol, top of line corrosion and steel microstructure are amongst those covered in the subsequent publications of de Waard et al. (de Waard and Lotz, 1993; de Waard and Milliams, 1975a, 1975b; de Waard et al., 1995, 1991). These new effects were accounted for by simply introducing additional empirical correction factors as multiplicators in the original de Waard and Milliams correlation. This transformed the original mechanistic approach of de Waard and Milliams into a semi-empirical model with all the disadvantages discussed above.

3.2. Elementary mechanistic models

The elementary mechanistic models were developed in attempt to address the shortcomings of empirical and semi-empirical corrosion rate prediction models and to bring the well-established general understanding of electrochemistry, chemistry and mass transfer into modeling. These models also formed the necessary platform required to further improve the mechanistic modeling of CO_2 corrosion. The elementary mechanistic models are based on a decoupled description of the main physicochemical phenomena involved in the corrosion processes, *i.e.* mass transfer,

charge transfer, and chemical reactions. These models derive their strength by relying on more descriptive electroanalytical data in their development (particularly steady state voltammograms), rather than the corrosion rate data alone. With this approach, the physicochemical parameters involved in various processes could be systematically studied. Unlike the correction factors used in empirical/semi-empirical models, the parameters used in elementary mechanistic models have a true theoretical meaning. Hence, the different elements of the model can be confidently combined in order to develop a model for more complex conditions.

The quantitative analysis of experimental results based on elementary mechanistic models provided the opportunity for deeper understanding of the underlying mechanisms. Additionally, such models for corrosion rate prediction offered flexibility for expansion to include more corrosive species, additional reactions and new physics, as well as allowing for more reliable extrapolation beyond the experimental conditions used in their development.

Gray et al. introduced one of the first and most comprehensive quantitative analyses of aqueous CO_2 corrosion of mild steel to date, by implementing an elementary mechanistic model for charge transfer rate calculations (Gray et al., 1990, 1989). Two consecutive studies were published by the authors in 1989 and 1990. The first article (Gray et al., 1989) focused on pH 4 in CO_2 saturated aqueous solution and the model is based on the direct carbonic acid reduction mechanism of de Waard and Milliams as discussed above. The model developed by Gray et al. uses Equation (11) for charge transfer calculations, and Equation (16) to account for the mass transfer limitation. The effect of the slow preceding CO_2 hydration reaction on direct carbonic acid reduction is included with an analogy to Equation (16) where the mass transfer limiting current is replaced with chemical reaction limiting current on rotating disk electrodes (Bard and Faulkner, 2001).

In their second publication (Gray et al., 1990), the test conditions were expanded toward more alkaline environments and higher temperatures. In that work, it was suggested that at pH values between 6 and 10 the bicarbonate ion reacts at the metal surface, similarly as carbonic acid does at lower pH values. In order to extend their mathematical model to higher temperature and pH values, including the bicarbonate reduction reaction, a similar approach as in their previous study (Gray et al., 1989) was used. However, the effects of additional physicochemical processes involved in these new conditions, such as formation of protective corrosion product layers (see chapter 4.2) were not considered in their second study.

Dayalan et al. (1995) took a slightly different approach in their calculation sequence compared to Grey et al., by implicitly equating the mass transfer and charge transfer rates (Equation (12)) at the metal surface in order to estimate the surface concentration of species. However, the model proposed in that study (Dayalan et al., 1995) does not include any temperature or CO_2 hydration reaction effects, and additionally, suffers from miscalculations in charge transfer rates. Despite these drawbacks, their approach was unique in the sense that it provides the first insight into the water chemistry at the corroding metal surface which is of significance for protective iron carbonate deposit formation calculations (Dayalan et al., 1998).

Another elementary mechanistic model of CO_2 corrosion was developed in a study published by Nesic et al. (1996a). In that work the authors developed a predictive mechanistic model based on the same elements introduced previously by Gray et al. (1990, 1989), while having a more practical implementation of the model for corrosion rate prediction in practical systems. Charge transfer rates are calculated based on Equation (11), mass transfer effect is based on Equation (14) to Equation (16), and the CO_2 hydration reaction was accounted for similarly to Gray et al. (1990, 1989). A different relationship for chemical reaction limiting current was used to accommodate for the effect of flow. Mass transfer correlations for different flow geometries were used, covering turbulent rotating cylinder flow and straight pipe flow (Nešić et al., 1995). The comparison of the results based on their model with linear sweep voltammograms, weight loss experiments was done to adjust the physicochemical parameters in the model. Additionally, a comparison of the performance of their model with the empirical/semi-empirical models of De Waard and Lotz (1993) as well as Dugstad et al. (1994) is provided by the authors.

Overall, the elementary mechanistic models gained general acceptance ever since, and have been widely used as the basis of mechanistic studies by many in the corrosion engineering field (Han et al., 2011a, 2011b, 2011c; Rajappa et al., 1998; Sundaram et al., 1996). However, the simple approach to implementation of physicochemical theory in the elementary mechanistic models discussed here suffers from one fundamentally flawed assumption. In these models it is assumed that species are transferred from the bulk fluid toward the metal surface and back independently from each other. In other words, the well-defined homogeneous chemical reactions as well as the ionic interaction (electromigration) between species inside the diffusion layer are ignored. While it can be argued that the latter effect can be insignificant in high conductivity solutions (aqueous brines), neglecting the chemical reactions disregards a significant process in these models. As an example, the *limiting current* in aqueous CO_2 environments was found to consist of two essential components: hydrogen ion mass transfer limiting current and CO_2 hydration reaction limiting current, which are considered to be additive in these models. While this results in a reasonable prediction of the corrosion rate as well as plausible voltammograms, it leads to inconsistent and in some cases flawed prediction of surface water chemistry. This is a crucial problem when trying to model important surface phenomena, such as adsorption of species and protective corrosion product formation or when trying to make more elaborate arguments about electrochemical corrosion mechanisms.

3.3. Comprehensive mechanistic models

Comprehensive mechanistic models were developed to be more true to the fundamental physicochemical laws that describe major processes involved in a corroding system in order to address some of the shortcomings of the elementary mechanistic models mentioned above. Additionally, these models bring significant advantages such as the unique insight into the possible reaction pathways and accurate estimation of species concentration at the metal surface.

This group of models refers to the mathematical models based on the solution of mass conservation equation in the diffusion layer (the Nernst–Planck equation). This approach has been introduced in CO_2 corrosion studies in the 1990s, while such calculations have been well established in the electrochemical engineering field in prior decades (Newman, 1973). Despite that the modeling approach is not novel by itself, the case of CO_2 corrosion can be considered as a rather complex application of such calculations.

The first mathematical model with this general approach was developed by Turgoose et al.(1992). In that study the authors developed a mathematical model based on the solution of the mass transfer equations and separately the homogeneous reaction equilibria of carbonate species in the diffusion layer. The potential of this type of modeling to provide detailed information about concentrations of species in the diffusion layer was demonstrated. It was shown that the various corrosion mechanisms proposed previously (de Waard and Milliams, 1975b; Schmitt and Rothmann,

1977; Więckowski et al., 1983a) are only limited interpretations of all the possible reaction pathways in aqueous CO_2 corrosion. However, the authors ignored the charge transfer kinetics of electroactive species and the model was only used to calculate the current response at mass transfer limiting condition.

A further improvement in comprehensive mechanistic modeling was introduced by Pots (1995). The model developed by Pots is based on Equation (18) where the convective mass transfer was calculated through empirical correlation for eddy diffusivity (Davies, 1972). In that work, charge transfer rates are assumed to follow the Tafel equation (Equation (11)) while the details of the parameters used in Tafel equation was not discussed. Pots also notes the significance of homogeneous reactions on the current response, suggesting that eliminating the direct reduction reaction of carbonic acid does not significantly alter the corrosion rates estimated by the model due to the parallel dissociation reaction.

In more extensive studies, Nesic et al. (2001) and Nordsveen et al. (2003) developed their model by implementing the Nernst–Planck (Equation (18)) to describe the mass transfer of species in the solution. The scope of the model was expanded beyond what was discussed in earlier works (Pots, 1995; Turgoose et al., 1992) by emphasis on the charge transfer rates calculations.

In charge transfer rate calculations used in comprehensive mechanistic models, Equation (16) is no longer valid and the mass transfer limitation effect is accounted for directly by calculating the surface concentration of species used in charge transfer rate expression. In order to accommodate this, Nesic et al. (2001) and Nordsveen et al. (2003) described the charge transfer kinetics through the Tafel equation (Equation (11)) while the bulk concentrations in exchange current densities (Equation (10) and Table 6) were replaced with surface concentrations. However, for this group of models, the proper charge transfer rate calculation should be based on Equation (6) where the surface concentrations are included in the ratio before the exponential term and the exchange current density is separately corrected for the variation in bulk concentration of active species (Table 6). For example, for the case of hydrogen ion reduction, the equation used by Nesic et al. (2001) and Nordsveen et al. (2003) shows a factor of $([H^+]_s/[H^+]_b)^{0.5}$ difference from what is given here by Equation (6) and in Table 6. Fig. 4 shows the ratio of hydrogen ion reduction current calculated by Nordsveen et al. (2003) and the one introduced here, versus the ratio $[H^+]_s/[H^+]_b$. Here, the $[H^+]_s/[H^+]_b$ ratio of unity corresponds to pure charge transfer controlled conditions where both relationships predict the same current. However, $[H^+]_s/[H^+]_b$ deviates from unity as the mass transfer limiting conditions becomes significant. Consequently, the charge transfer rates calculated by the two relationships deviate notably. On the other hand, at pure mass transfer limiting conditions, where the kinetics of charge transfer is insignificant in the observed current densities, a similar limiting current would be obtained but corresponding to different surface concentrations. The deviation showed in Fig. 4 is therefore only significant in the mixed control region.

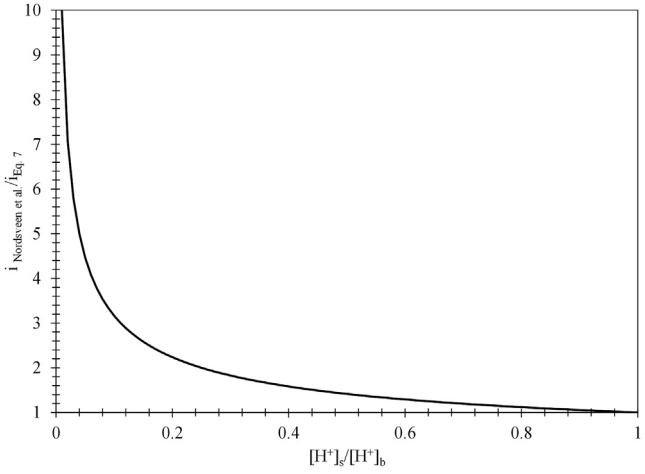

Fig. 4. Comparison of the current calculated from the charge transfer expression used by Nordsveen et al. (2003) for hydrogen ions reduction and the relationships provided as Equation (6) and Table 6 at 298 K and pH 4. The vertical axis represents normalized surface concentration of hydrogen ions.

The charge transfer rate calculation expressions similar to those by Nordsveen et al. (2003), were also used later in several subsequent studies (Choi et al., 2013; Kittel et al., 2013; Remita et al., 2008; Song, 2010; Song et al., 2004; Tribollet et al., 2014).

In a more recent study, Remita et al. (2008) revisited the mechanism of CO_2 corrosion, using a similar approach to quantify their experimental data. The model used in that work is the simplified steady state form of the model proposed by Nordsveen et al. (2003), *i. e*, the left hand side of Equation (20) was taken to be zero. Using a steady state form of the models discussed above may be sufficient for practical purposes of corrosion rate estimation and also to compare with steady state voltammograms. This approach benefits from the comprehensive treatment of the homogeneous chemical reactions in the diffusion boundary layer and is computationally more affordable. However, the charge transfer rates in the work of Remita et al. (2008) are calculated similar to Nesic et al. (2001) and Nordsveen et al. (2003) suffering from the same issue as described above.

The comprehensive mechanistic models discussed here have demonstrated their strength by depicting a more detailed and accurate picture of the processes involved in corrosion of steel in CO_2 environments. Such models are better suited to serve as a basis for further studies and a more appropriate platform for description of more complex systems and inclusion of new processes (some examples described in the section below). On the other hand, they are significantly more complicated to construct and use. Therefore, the much simpler elementary mechanistic models are still more popular with the corrosion engineers and even within the academic community, despite the known shortcomings.

4. Extension beyond basic calculations

One of the main qualities of any given corrosion modeling approach is its ability to be extended to cover more complex conditions and to have additional species and processes incorporated into the base model. The flexibility of models to include *additional corrosive species* is discussed below using the examples of acetic acid and hydrogen sulfide. The ability of the models to incorporate additional physicochemical phenomena is discussed below by using the example of *protective corrosion product film formation*. Finally, *top of the line corrosion* (TLC) encountered in wet gas pipelines is used to illustrate the flexibility of the models to be adapted for an application with very different geometry, environment, and physical and chemical conditions.

4.1. Additional corrosive species

The ability of a corrosion rate predictive model to incorporate new species is of great interest for practical applications where the water chemistry is more complex compared to laboratory experiments. Hydrogen sulfide and organic acids are two main additional corrosive species commonly found in the aqueous solution alongside carbonic acid. The water chemistry associated with these weak acids can be accounted for in a similar way to what was discussed earlier for CO_2.

Reports on the significant effect of acetic acid in pipeline

corrosion in oil and gas industry are found as early as 1940s, where it was shown that even in concentrations as low as 300 ppm, acetic acid can cause severe corrosion of pipeline steel (Menaul, 1944). Similar to the carbonic acid corrosion, the mechanism of acetic acid corrosion has been intensely debated in the last two decades. While many studies suggest that the increased corrosion rates in the presence of acetic acid is due to its direct reduction at the metal surface (Fajardo et al., 2007; Garsany et al., 2002; George and Nešic, 2007; Gulbrandsen and Bilkova, 2006; Matos et al., 2010; Okafor et al., 2009; Sun et al., 2003), others suggest that acetic acid corrosion follows the buffering effect mechanism (Amri et al., 2011, 2009; George et al., 2004; Hurlen et al., 1984; Pots et al., 2002; Tran et al., 2013).

Corrosion of mild steel by aqueous hydrogen sulfide has also been extensively investigated in the last few decades. It was recently confirmed that hydrogen sulfide follows the direct reduction mechanism based on clear observation of a distinct additional wave in cathodic sweeps (Kittel et al., 2013; Tribollet et al., 2014; Zheng et al., 2014).

In order to include the effect of additional corrosive species in empirical/semi-empirical models, extensive experimental and computational work is required, with no clear prospects of success. In order to maintain the same level of performance, the data pool on which the model was previously built needs to be extended to cover the effect of new species on the corrosion rates over the whole range of physical conditions such as temperature, flow conditions, CO_2 partial pressures, etc. This is usually a very difficult if not an impossible task. Additionally, the model itself and the correction factors have to be redefined to accommodate for such an expansion, without any proper theoretical guidance.

On the other hand, the elementary mechanistic models as well as the comprehensive mechanistic models easily cope with such expansions. New species are included by introducing additional charge transfer, chemical and mass transfer equations into the core model, describing the new species and processes, as appropriate. The corresponding physicochemical parameters are obtainable with a relatively small number of additional targeted experiments. In elementary mechanistic models, for each additional electroactive species, one extra equation (Equation (16)) is added to the model and solved simultaneously with the existing equations. An example of such an extension for an elementary mechanistic model is provided in Fig. 5 by introducing acetic acid effect into the existing CO_2 corrosion model.

In the comprehensive mechanistic models, each new species is included by adding its corresponding Nernst–Planck equation (Equation (20)) into the model. If those species are involved in chemical reactions with any of the other species, this is defined via the chemical reaction term in the Nernst–Planck equation. Similar to elementary mechanistic models, additional physicochemical constants in comprehensive mechanistic models can also be defined by a limited number of targeted experiments. As an example, Fig. 6 shows the normalized concentration profiles of the active species within the diffusion layer at the corrosion potential, demonstrating the effect of acetic acid, as the additional corrosive species, when added to a comprehensive mechanistic CO_2 model.

4.2. Effect of corrosion product layer

The corrosion process is often accompanied by corrosion product layer formation at the metal surface. The protectiveness, chemical composition, as well as mechanical and physical properties of this precipitated layer are greatly affected by water chemistry, environmental conditions such as temperature and fluid flow, steel composition and microstructure, etc. (Crolet et al., 1999; Davies and Burstein, 1980; Dugstad, 1998; Gulbrandsen, 2007; Johnson and Tomson, 1991; Kermani and Morshed, 2003; Ruzic et al., 2007; Sun et al., 2009; van Hunnik et al., 1996). This may lead to complex, multi-layer corrosion product precipitates (Choi et al., 2014; Farelas et al., 2014; Pfennig and Bäßler, 2009; Pfennig and Kranzmann, 2011, 2009). By limiting the discussion to CO_2 corrosion of carbon steel at conditions typical for transmission lines, one only encounters a porous iron carbonate corrosion product layer. This scenario has been incorporated in the mechanistic models (Anderko, 2000; Dayalan et al., 1998; Nešić and Lee, 2003; Nordsveen et al., 2003; Rajappa et al., 1998; Sundaram et al., 1996). It is worth noting that the models listed above neglect the effect of steel microstructure resulting in the formation of an iron carbide network, although it has been shown that it may affect the formation of iron carbonate (Farelas et al., 2010).

The precipitation/dissolution of iron carbonate is described through the following heterogeneous chemical equilibrium:

$$Fe^{2+} + CO_3^{2-} \rightleftharpoons FeCO_{3(s)} \tag{24}$$

If the product of the concentration of species on the left hand side exceeds the saturation limit, the formation of iron carbonate deposit by precipitation is favored. The formation of porous corrosion product layer on the metal surface affects the corrosion

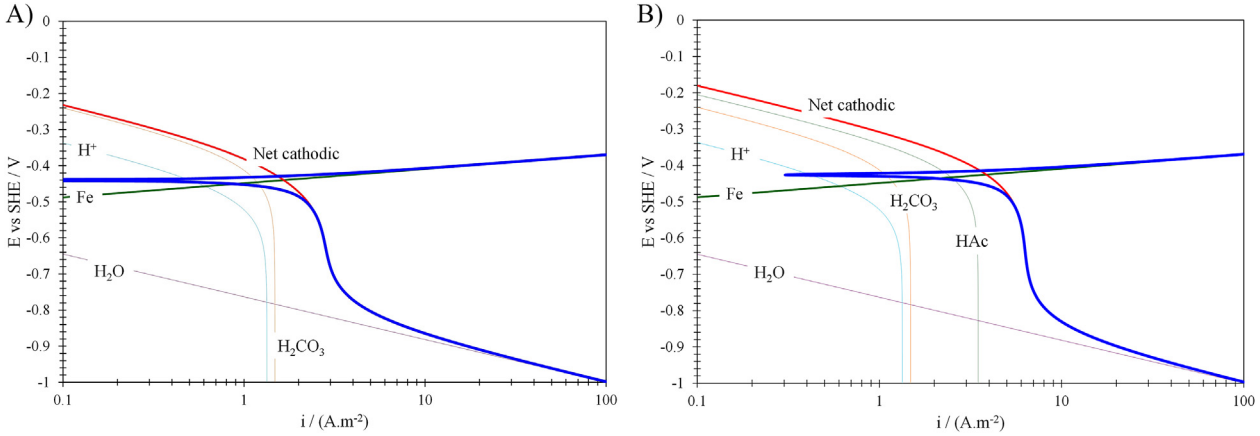

Fig. 5. Predicted voltammograms (solid blue line) by FREECORP (Nešić et al., 2009) at pH4, 25 °C, 1 bar CO_2, and 1 m/s flow velocity. A) 0 ppm acetic acid and B) 100 ppm acetic acid (HAc).

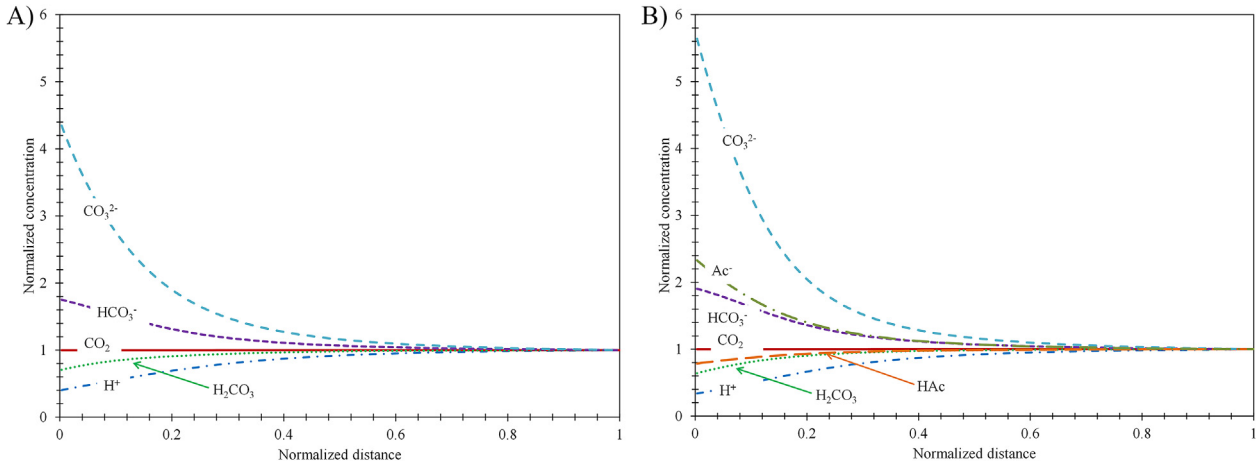

Fig. 6. Predicted concentration profile by MULTICORP™ at pH4, 25 °C, 1 bar CO_2, and 1 m/s flow velocity. A) 0 ppm acetic acid and B) 100 ppm acetic acid (HAc).

process through two main mechanisms:

- The porous iron carbonate layer acts as a barrier against transport of chemical species toward and away from the metal surface.
- The porous iron carbonate corrosion product layer blocks portions of the metal surface, making them unavailable as reaction sites.

Formation of a protective iron carbonate layer in CO_2 corrosion of steel is best discussed in the context of two general criteria, one thermodynamic, the other kinetic (van Hunnik et al., 1996).

A thermodynamic indicator for the precipitation process is described by the extent of departure from equilibrium (Reaction 24), termed here: the saturation value (S_{FeCO3}):

$$S_{FeCO_3} = \frac{C_{Fe^{2+}} C_{CO_3^{2-}}}{K_{sp}} \tag{24}$$

where K_{sp} is iron carbonate dissolution equilibrium constant (Sun et al., 2009) for Reaction 24. A high saturation value is not the only factor leading to protective layer formation, because properties of an iron carbonate layer such as density, porosity, and adherence to the metal surface are greatly affected by kinetics of iron carbonate precipitation (Dugstad, 1998; van Hunnik et al., 1996). Additionally, the protectiveness of the corrosion product layer can be influenced by various chemical and mechanical removal processes (Ruzic et al., 2007, 2006a, 2006b). However, the formation of the iron carbonate layer does not completely stop the corrosion process, this causes the existing corrosion product layer to detach from the metal surface (Pots and Hendriksen, 2000; van Hunnik et al., 1996). This process, known as “film undermining” (Nešić and Lee, 2003), affects the adherence, density and porosity of the corrosion product layer and ultimately its protectiveness. The role of undermining was quantified by van Hunnik et al. (1996) through the introduction of a kinematic parameter called “scaling tendency” as described by Equation (25). Scaling tendency can also be seen as a practical measure to assess the protectiveness and the ability to repair a damaged iron carbonate layer (Gulbrandsen, 2007; Sun and Nesic, 2006; van Hunnik et al., 1996).

$$ST = \frac{R_{FeCO_{3(s)}}}{CR} \tag{25}$$

A scaling tendency of ST << 1 represents the case where the undermining is much faster than the formation of the corrosion product layer, therefore, a porous, often thick and non-protective layer forms, even at high saturation values. On the other hand a scaling tendency of ST >> 1 suggests that the undermining is overpowered by the rapidly forming iron carbonate precipitate, creating a dense protective layer (Nešić and Lee, 2003; Sun and Nesic, 2006).

As for any crystalline deposits, the formation of iron carbonate should be discussed in the context of crystal nucleation and crystal growth (Lasaga, 1998). Johnson and Tomson (1991) studied the rate of iron carbonate formation using the iron count method to evaluate the iron carbonate growth rate on seed particles dispersed in the bulk solution. Based on their experimental approach of using seed particles at low saturation values (<2), authors bypassed the nucleation step and proposed a precipitation rate purely based on the crystal growth kinetics. Van Hunnik et al. (1996) argued that the saturation values considered in Johnson and Tomson (1991) precipitation rate expression does not cover an adequate range for CO_2 corrosion applications and may result in significant over estimation of precipitation rates. Van Hunnik et al. therefore used experimental data with saturation values as high as 1000, while the same indirect measurements method as Johnson and Tomson (1991) was utilized to calculate the precipitation rates. In this study authors investigated the precipitation of iron carbonate on a corroding metal surface rather than iron carbonate seeds, thus both nucleation and crystal growth step were involved. However, authors suggested that the crystal growth is the dominant process controlling the net precipitation rate. The ability of the expression they proposed to predict the precipitation rate, regardless of the steel microstructure, was considered as the proof of such an argument. This subject was also revisited by Sun and Nešić (2008), where the previous expressions (Johnson and Tomson, 1991; van Hunnik et al., 1996) were shown to over-predict the precipitation rate. The authors implemented a direct measurement of $FeCO_3$ precipitation rates through mass gain on steel samples. Similar to van Hunnik et al. (1996), this experimental approach included both nucleation and growth mechanisms. However, authors suggest that in the case of iron carbonate formation on a heterogeneous mild steel substrate, the net precipitation rate is governed by crystal growth mechanism as the rate determining step. Despite the arguments provided by various authors (Johnson and Tomson, 1991; Sun and Nešić, 2008; van Hunnik et al., 1996), concerns related to change in saturation level over the duration of the experiments, effect of mass transfer, the mechanism of the precipitation/dissolution reaction, and disregarding the kinetics of nucleation step, demand further investigations.

Table 7
Summary of the precipitation rate expressions.

Reference	$f(T)$	$g(S_{FeCO_3})$	K_{sp}
Johnson and Tomson (1991)	$exp(54.8 - \frac{-123000}{RT})$	$K_{sp}(S_{FeCO_3}^{0.5} - 1)^2$	$exp(-36.22 - \frac{-30140}{RT})$
van Hunnik et al. (1996)	$exp(52.4 - \frac{-119800}{RT})$	$K_{sp}(S_{FeCO_3} - 1)(1 - S_{FeCO_3}^{-1})$	Not specified
Sun and Nesic (2008)	$exp(21.3 - \frac{-64851.4}{RT})$	$K_{sp}(S_{FeCO_3} - 1)$	(Sun et al., 2009)

The precipitation rate of iron carbonate in Equation (25) can be described by an expression in general form of Equation (26) (Lasaga, 1998).

$$R_{FeCO_{3(s)}} = \frac{A}{V} f(T) g(S_{FeCO_3}) \tag{26}$$

where

$$f(T) = e^{\left(A - \frac{B}{RT}\right)} \tag{27}$$

represents the rate constant as a function of temperature based on Arrhenius' equation where constants A and B are determined empirically. The precipitation rate dependence on saturation value is accounted for by the $g(S_{FeCO3})$ function that is defined by the mechanism of the precipitation/dissolution reaction. For an elementary reaction this function can be theoretically expressed as Equation (28) (Lasaga, 1998).

$$g(S_{FeCO_3}) = K_{sp}(S_{FeCO_3} - 1) \tag{28}$$

This equation is similar to what was proposed by Sun and Nesic (2008) indicating that the precipitation reaction follows a first order reaction kinetics. The more elaborate forms of the function $g(S_{FeCO3})$, such as the ones introduced by van Hunnik et al. (1996) and Johnson and Tomson (1991) may suggest a more complex mechanism for this reaction (Table 7). The lack of mechanistic discussions categorizes these two precipitation rate equations as semi-empirical expressions with all of their intrinsic limits. A summary of the expressions for precipitation rate proposed by the abovementioned references is provided in Table 7.

In the case of elementary mechanistic models, the effect of a protective iron carbonate layer was accounted for by introducing an additional mass transfer resistance layer (Dayalan et al., 1998; Rajappa et al., 1998; Sundaram et al., 1996), without accounting for the surface blocking effect. A composite mass transfer resistance at quasi steady state condition as well the interfacial concentrations of species can be obtained in order to calculate the corrosion rate. However, considering the aforementioned issue of the elementary mechanistic models which disregard the chemical reactions in the diffusion layer, the accuracy of this approach is questionable. Additionally, while being simple to implement, this approach further suffers from the fact that the thickness and porosity of a protective iron carbonate layer must be specified in advance of any corrosion rate calculation. As this is usually not known, an additional empirical correlation is needed, relating the properties (protectiveness) of a protective iron carbonated layer to environmental conditions.

The comprehensive mechanistic models can also be readily adapted to account for the effect of a precipitated corrosion product layer. In this case, the Nernst Planck equation is rewritten as (Nešić et al., 2001; Nordsveen et al., 2003):

$$\frac{\partial(\varepsilon C_i)}{\partial t} = -\nabla \cdot \left(\varepsilon^{3/2} N_i\right) + \varepsilon R_i \tag{29}$$

in order to account for mass transfer through a porous media, with a porosity ε. In the portion of the boundary layer away from the steel surface where there is no iron carbonate layer the porosity ε is equal to one. Furthermore, all electrochemical rate expressions (current densities) are modified by multiplying with surface porosity ε, in order to account for the surface blocking effect. While these models benefit from accurate surface concentration calculations, the distribution of porosity in the precipitating iron carbonate layer still needs to be defined properly. In a simplistic approach it could be described by an empirical function in the same way as it is done for the elementary models (Nešić et al., 2001).

In a more comprehensive approach, Nesic et al. presented a model for calculation of porosity distribution in the iron carbonate layer (Nešić et al., 2003, 2002). The authors proposed that the porosity can be calculated by writing a mass balance for the solid iron carbonate precipitate as:

$$\frac{\partial \varepsilon}{\partial t} = -\frac{M_{FeCO_3}}{\rho_{FeCO_3}} R_{FeCO_3} - CR\frac{\partial \varepsilon}{\partial x} \tag{30}$$

where the first term is related to precipitation kinetics (Equation (26)) and the second (convective-like) term arises from the undermining effect, described above. This approach is equivalent to using the concept of scaling tendency, but one that is based on local concentrations at the steel surface and in the porous iron carbonate layer, rather than basing it on bulk concentrations. This equation needs to be solved simultaneously with Equation (29) for all the other species in order to provide an estimate of the porosity distribution within the corrosion product layer, and account for the effect it has on concentrations and fluxes of all other species and ultimately on the corrosion rate.

Fig. 7 shows the comparison of the calculated results with the experimental data from (Nešić and Lee, 2003). The estimated profile of corrosion product layer porosity shows good qualitative agreement with the SEM image, where a dense precipitate is found with the part closer to the metal surface appearing to be more porous. However, as discussed by the authors, the estimated corrosion product layer thickness lacks accuracy at some of the conditions, which could be due imprecise kinetics or due to a removal processes via mechanical destruction as well as chemical dissolution (Ruzic et al., 2007, 2006a, 2006b), which are not considered in the model.

4.3. Top of the line corrosion

An example that illustrates the ability of comprehensive models to be extended relatively easily to cover quite different corrosion scenarios is the implementation for Top of the Line Corrosion (TLC) prediction.

TLC is a corrosion phenomenon occurring in pipeline transportation of wet gas when there is a significant difference of temperature between the produced fluids and the surrounding environment. If the gas/liquid flow is stratified, warm saturated water vapor condenses on the inside walls of the pipeline and forms small water droplets which become saturated with acid gases, thus leading to severe corrosion issues (Ruhl and Kranzmann, 2013, 2012; Singer et al., 2013). There is no simple mitigation method available, especially considering that the use of

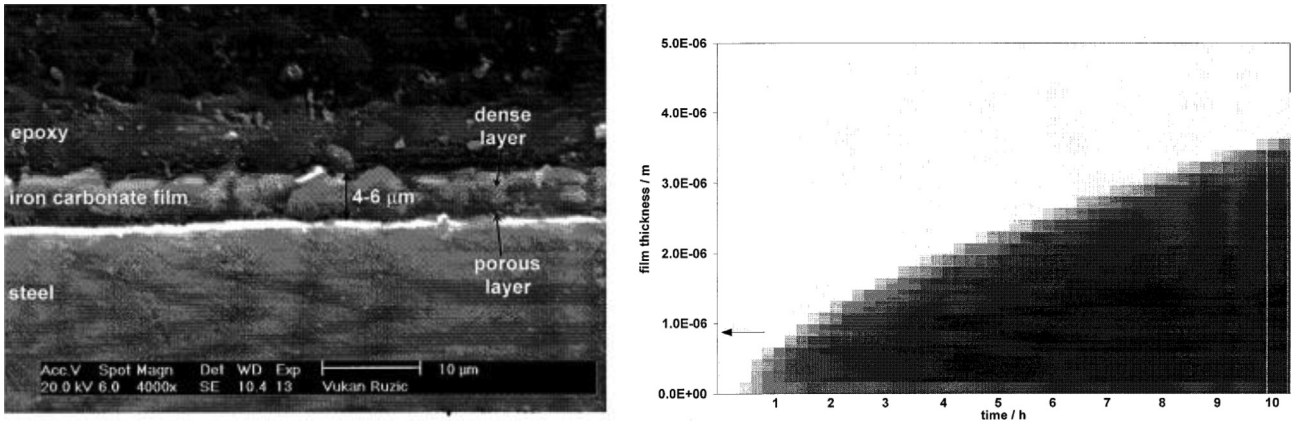

Fig. 7. SEM image of the corrosion product layer cross section formed after 10 h at T = 80 °C, pH = 6.6, P_{CO2} = 0.54 bar, ferrous ion concentration of 250 ppm, and v = 1 m/s. The graph at right shows the calculated porosity profile along the film thickness of the iron carbonate layer depicted in different shades of gray in similar conditions where white corresponds to ε = 1 and black is ε = 0 (Nešić and Lee, 2003). [2]

standard corrosion inhibitors is not feasible as they cannot readily reach the top portions of the pipeline.

TLC is very dependent on the rate of water condensation, temperature, and the solubility of corrosion products but is also linked to the presence of CO_2 and organic acids. Only a limited number of sour TLC cases have also been reported (Bich and Szklarz, 1988; Joosten et al., 2010; Paillassa et al., 1963), and will not be discussed here. A key aspect of understanding the TLC mechanism is the interaction between condensation, corrosion, the evolution of the chemistry in the condensed water and formation of the corrosion product layers (iron carbonate). The size of the water droplet is controlled by the condensation rate (leading to an increase in droplet size) and by gravity and drag forces (leading to removal of droplets from the pipe wall). Corrosion products can accumulate rather quickly in the water phase leading to supersaturation with regard to iron carbonate. The formed corrosion product layer tends to block the steel surface and act as a mass transfer barrier and thus decrease the corrosion rate. However, the water in the droplet is constantly re-supplied by pure condensed water, which tends to dilute the corrosion products and decrease the saturation value. The understanding of TLC mechanisms, lies in the balance between the corrosion process, which leads to supersaturation and precipitation of iron carbonate, and the condensation process, which tends to decrease the iron carbonate saturation level and lead to dissolution of the corrosion product layer (Nyborg and Dugstad, 2007; Pots and Hendriksen, 2000).

The example of TLC is interesting for the present discussion, since there are actually no new physicochemical processes involved when compared to standard "bottom of the line" corrosion described above, other than water condensation and droplet formation. The same chemical and electrochemical processes discussed previously are valid. This is also true for the mechanism of iron carbonate precipitation. Therefore, adapting the existing mechanistic CO_2 corrosion models to the TLC environments is relatively straightforward, while this would not be the case for empirical or semi-empirical models.

Several empirical/semi-empirical approaches have been proposed to model TLC. De Waard et al. (1991) were the first to propose a model for TLC based on a correction for his widely used semi-empirical corrosion prediction equation. De Waard et al. introduced a correction factor: $F_{cond} = 0.1$ in order to adapt his model to condensation conditions which was to be valid for condensation rates below an experimentally determined "critical" rate of 0.25 mL m^{-2}. s^{-1}.

In 2000, a different model was proposed by Pots and Hendriksen (2000) which aimed at accounting for the competition between the iron carbonate layer precipitation rate and the condensation rate. The so called "supersaturation model" is based on the calculation of ferrous ion concentration at saturation under precipitating conditions. The steady state corrosion rate was described based on the flux of ferrous ion required to keep the condensed water supersaturated, shown by Equation (31). The ferrous ion concentration used in Equation (31) was obtained by calculating the saturation value from equating corrosion rate (*CR*) with the precipitation rate (Table 7).

$$CR = 10^6 \times 24 \times 3600 \times 365 \frac{M_{Fe}}{\rho_{Carbonsteel}} C_{Fe^{2+},sat} \frac{WCR}{\rho_{H_2O}} \quad (31)$$

Pots and Hendriksen emphasized the importance of correctly evaluating the condensation rate and characterizing the chemistry of the aqueous phase in order to accurately predict the corrosion rate.

More recently, Nyborg and Dugstad (2007) developed another semi-empirical equation for TLC prediction based on their own experimental work. It is hinged on the concept that TLC is limited by the amount of iron which can be dissolved in the thin film of condensing water. According to Nyborg and Dugstad, the TLC rate can be modeled as being proportional to the water condensation rate, the iron carbonate solubility, and supersaturation value. Although no detail are provided on how the condensation rate is calculated, authors stressed the importance of predicting an accurate condensation rate, as it will have a much more pronounced effect on TLC than, for example, the CO_2 partial pressure. The semi-empirical equation of Nyborg and Dugstad is shown below and is valid only for low acetic acid content (<0.001 M), low to medium CO_2 partial pressure (<3 bars) and no H_2S:

$$CR = 0.004 \times 10^9 \times C_{Fe^{2+},sat} M_{Fe} WCR(12.5 - 0.09(T - 273.15)) \quad (32)$$

Still, all these attempts suffer from the usual shortcomings

[2] Reproduced with permission from NACE International, Houston, TX. All rights reserved. S. Nešic, K.L.J. Lee, A mechanistic model for carbon dioxide corrosion of mild steel in the presence of protective iron carbonate films-Part 3: Film growth model, Corrosion, 59, 7, 2003. ©NACE International 1945.

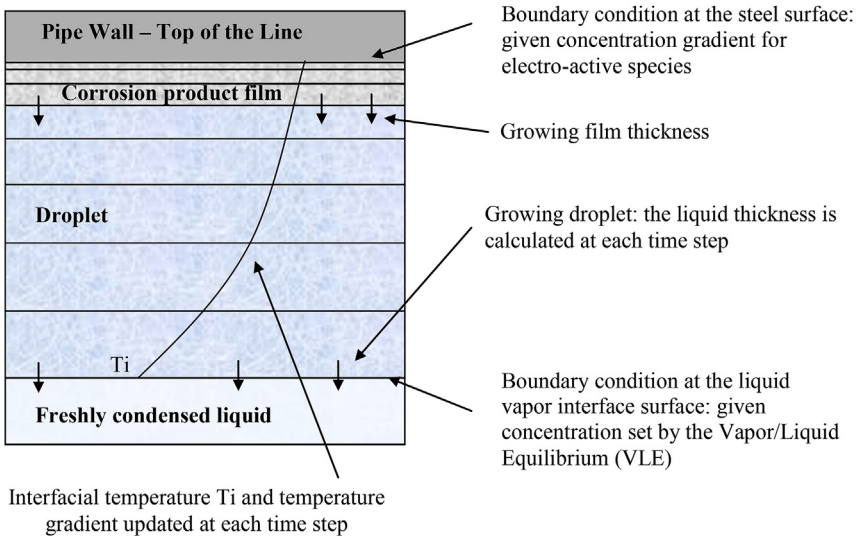

Fig. 8. Schematic of the corrosion calculations in a growing droplet simulated as a one-dimensional film (Singer, 2013).

associated with empirical and semi-empirical models, *i.e.* they have limited ability to extrapolate beyond the range of parameters they have been developed for and cannot be easily adapted to take into account additional influencing parameters such as, new species or additional types of corrosion products.

Zhang et al. (2007) published the first fully comprehensive mechanistic approach to TLC modeling. The key point for this discussion is that this model was directly adapted from the mechanistic CO_2 corrosion approach developed by Nordsveen (2003) and Nesic et al. (Nešić and Lee, 2003; Nešić et al., 2003, 2001). As mentioned before, the underlying mechanisms of corrosion (chemistry in the condensed water and the corrosion at the steel surface) have not been changed when adapting them to TLC. The only real change was the implementation of dropwise condensation rate prediction, based on the heat and mass transfer theory (Zhang et al., 2007). The boundary conditions specific to TLC scenario have also to be implemented. Zhang et al. stated that, from a statistical point of view, every point on the metal surface has the same probability of being covered by liquid droplets and, consequently, it can be assumed that the entire surface is subject to uniform corrosion. This simplifies the mathematical approach from a three-dimensional situation (with semi-hemispherical droplet) to a one-dimensional geometry (in the shape of a finite liquid film), as shown in Fig. 8. The droplet growth and loss is simulated by an increase in the liquid film with time until it reaches a calculated maximum size where the droplet disappears (falls or slides). The calculation then restarts with a minimum water film thickness (corresponding to the minimum droplet size), and the cycle is repeated, until the corrosion process reaches a steady state. Another easy adjustment of the standard "bottom of the line" corrosion model was the absence of the supporting electrolyte (salt) and ignoring the effect of flow on mass transfer within the water film.

Zhang's approach is a good example showing the adaptability of comprehensive models. The model validity range is extended by improving the physical representations of the relevant physico-chemical phenomena. Other extension can be readily made by for example broadening the temperature and pressure validity ranges for kinetics or equilibrium constants, etc. New species and additional corrosion products can be easily added as the knowledge of the underlying corrosion mechanism matures.

5. Conclusions

Corrosion rate predictive models of mild steel in the presence of dissolved CO_2 have improved significantly since initial studies appeared in the mid 1970s. Driven by economical, safety and environmental concerns, numerous studies and mathematical models are now available pertaining to this system. In this review, mathematical models have been categorized into three main groups: empirical/semi-empirical, elementary mechanistic, and comprehensive mechanistic models. The mechanistic models show a much better potential for further development to cover more complex conditions; they offer transparency, flexibility, and extrapolation capabilities in a way that empirical/semi-empirical models cannot.

The state of the art models in CO_2 corrosion are comprehensive mechanistic models which benefit from an inclusive theoretical treatment. These models offer greatest flexibility to be adopted to cover various conditions and corrosion scenarios by adding new physics, as the knowledge of the underlying mechanisms becomes mature. Nevertheless, many challenges persist, such as improved kinetics of underlying electrochemical reactions, better understanding of protective corrosion product layer growth, extension to sour conditions, etc., which are all subject of current research efforts.

In spite of that, comprehensive mechanistic models offer the most flexible platform for inclusion of new and more complex phenomena encountered in practical applications, such as the effect of steel microstructure, effect of alloying compounds, application of inhibitors, modeling of localized attacks, etc.

Acknowledgment

The authors would like to acknowledge the financial support from Anadarko, Baker Hughes, BP, Chevron, Clariant Oil Services, CNPC Tubular Goods Research Center, ConocoPhillips, DNV GL, Hess, INPEX Corporation, M-I SWACO (Schlumberger), Multi-Chem (Halliburton), Nalco Champion, Occidental Oil Company, Petrobras, Petroleum Development Oman, Petroleum Institute (Gas Research Center), Petronas, PTT, Saudi Aramco, SINOPEC (China Petroleum), TransCanada, TOTAL, and Wood Group Integrity Management under joint industrial research project. The authors are also grateful for constructive comments and discussions with D. Young, S. Hassani, and B. Brown.

Nomenclature

A	Active surface area of the deposit, m^2
α_j	Transfer coefficient of electrochemical reaction j, –
b	Tafel slope, V
CR	Corrosion rate, mm yr^{-1}
C_i	Concentration of species i, M
C_i^s	Concentration of species i at the electrode surface, M
C_i^b	Concentration of species i in the bulk solution, M
$C_{i,ref}^b$	Concentration of species I in the bulk solution at reference conditions, M
$C_{Fe^{2+},sat}$	Concentration of Fe^{2+} in the bulk solution at saturation with regard to $FeCO_3$, M
D	Pipe/sample diameter, m
D_i	Diffusion coefficient of species i, m^2 s^{-1}
$D_{i,lim}$	Diffusion coefficient of the limiting species, m^2 s^{-1}
δ	Diffusion layer thickness, m
E	Electrode potential, V
E^0	Standard potential, V
E_{rev}	Reversible potential, V
E_a	Activation energy, J mol^{-1}
ε	Porosity, –
η	Over potential, V
F	Faraday's constant, C mol^{-1}
H_{CO_2}	Henry's constant of CO_2, M bar^{-1}
i	Current density, A m^{-2}
$i_{0,j}$	Exchange current density of reaction j, A m^{-2}
$i_{0,j,ref}$	Exchange current density of reaction j at reference conditions, A m^{-2}
i_{lim}	Mass transfer limiting current density, A m^{-2}
i_{ct}	Charge transfer controlled current density, A m^{-2}
i_{net}	Net current density, A m^{-2}
i_{corr}	Corrosion current density, A m^{-2}
K_j	Equilibrium constant of reaction j, Varies
K_{sp}	Dissolution equilibrium constant, Varies
$K_{0,j}$	Standard reaction rate constant of electrochemical reaction j, Varies
k_0	Pre-exponent term in Arrhenius' equation, Varies
k_j	*R*eaction rate constant of reaction j, Varies
k_m	Mass transfer coefficient, m s^{-1}
L	Characteristic length, m
m	Reaction order, –
M_i	Molecular weight of species i, g mol^{-1}
μ	Viscosity, N s m^{-2}
n	Number of electrons transferred, –
N_i	Flux of species i, mol m^{-2} s^{-1}
υ	Kinematic viscosity, M^2 s^{-1}
Ω	Rotation speed, Rad s^{-1}
p_i	Partial pressure of species i, bar
ϕ	Potential in the solution, V
R	Universal gas constant, j mol^{-1} K^{-1}
Re	Reynolds number, –
R_i	Rate of chemical reaction of species i, M s^{-1}
ρ_i	Density of species i, kg m^{-3}
$S‰$	Salinity, g(salt) kg^{-1}(solution)
S_{FeCO_3}	Saturation value of $FeCO_3$, –
Sh	Sherwood number, –
Sc	Schmitt number, –
ST	Scaling tendency, –
T	Temperature in kelvin, K
T_{ref}	Temperature in kelvin at reference conditions, K
T_c	Temperature in centigrade, C
t	Time, s
u_i	Mobility of species i, m^2 V s^{-1}
V	Volume of the deposit, m^3
v_x	Fluid velocity along × axis, m s^{-1}
WCR	Water condensation rate, kg m^{-2} s^{-1}
x	Normal distance from electrode surface, m
z_i	Electrostatic charge of species i, –

References

Amri, J., Gulbrandsen, E., Nogueira, P.R., 2009. Effect of Acetic Acid on Propagation and Stifling of Localized Attacks in CO_2 Corrosion of Carbon Steel. NACE International. Paper No. 284.

Amri, J., Gulbrandsen, E., Nogueira, R.P., 2011. Role of Acetic Acid in CO_2 Top of the Line Corrosion of Carbon Steel. Nace International. Paper No. 329.

Anderko, A., 2010. Shreir's Corrosion. Elsevier. http://dx.doi.org/10.1016/B978-044452787-5.00083-4.

Anderko, A., 2000. Simulation of $FeCO_3$/FeS scale formation using thermodynamic and electrochemical models. In: Corrosion 2000. Paper No. 102.

Aravinth, S., 2000. Prediction of heat and mass transfer for fully developed turbulent fluid flow through tubes. Int. J. Heat Mass Transf. 43, 1399–1408. http://dx.doi.org/10.1016/S0017-9310(99)00218-5.

Bard, A.J., Faulkner, L.R., 2001. Electrochemical Methods: Fundamentals and Applications. John Wiley & Sons, INC. http://dx.doi.org/10.1016/j.aca.2010.06.020.

Bich, N.N., Szklarz, K.E., 1988. Crossfield Corrosion Experience. Nace International. Paper No. 196.

Bockris, J.O., Ammar, I.A., Huq, A.K.M.S., 1957. The mechanism of the hydrogen evolution reaction on platinum silver and tungsten surfaces in acid solutions. J. Phys. Chem. 61, 879–886. http://dx.doi.org/10.1021/j150553a008.

Bockris, J.O., Drazic, D., Despic, A.R., 1961. The electrode kinetics of the deposition and dissolution of iron. Electrochim. Acta 4, 325–361. http://dx.doi.org/10.1016/0013-4686(62)87007-8.

Bockris, J.O., Drazic, D., Despic, A.R., 1962. The kinetics of deposition and dissolution of iron: effect of alloying impurities. Electrochim. Acta 7, 293–313. http://dx.doi.org/10.1016/0013-4686(62)87007-8.

Bockris, J.O., Koch, D.F.A., 1961. Comparative rates of the electrolytic evolution of hydrogen and deuterium on iron, tungsten and platinum. J. Phys. Chem. 65, 1941–1948.

Bockris, J.O., McBreen, J., Nanis, L., 1965. The hydrogen evolution kinetics and hydrogen entry into α-iron. J. Electrochem. Soc. 112, 1025–1031. http://dx.doi.org/10.1149/1.2423335.

Bockris, J.O., Potter, E.C., 1952. The mechanism of the cathodic hydrogen evolution reaction. J. Electrochem. Soc. 99, 169. http://dx.doi.org/10.1149/1.2779692.

Bockris, J.O., Reddy, A.K.N., 1973. Modern Electrochemistry: an Introduction to an Interdisiplinary Area, vol. 2. Plenum Press, New york.

Brug, G.J., Sluyters-Rehbach, M., Sluyters, J.H., Hemelin, A., 1984. The kinetics of the reduction of protons at polycrystalline and monocrystalline gold electrodes. J. Electroanal. Chem. 181, 245–266. http://dx.doi.org/10.1016/0368-1874(84)83633-3.

Butler, J.N., 1991. Carbon Dioxide Equilibria and Their Applications. CRC Press.

Chin, R.J., Nobe, K., 1972. Electrodissolution kinetics of iron in chloride solutions III. Acidic solutions. J. Electrochem. Soc. 119, 1457–1461. http://dx.doi.org/10.1149/1.2408267.

Choi, Y., Duan, D., Jiang, S., Nešić, S., 2013. Mechanistic modeling of carbon steel corrosion in a methyldiethanolamine (MDEA)-based carbon dioxide capture process. Corrosion 69, 551–559.

Choi, Y.-S., Farelas, F., Nešić, S., Magalhães, A.A.O., de Azevedo Andrade, C., 2014. Corrosion behavior of deep water oil production tubing material under supercritical CO_2 environment: part 1—effect of pressure and temperature. Corrosion 70, 38–47. http://dx.doi.org/10.5006/1019.

Coney, M.W.E., Board, G.B.C.E.G., 1981. Erosion-corrosion: the Calculation of Mass-transfer Coefficients.

Conway, B.E., Tilak, B.V., 2002. Interfacial processes involving electrocatalytic evolution and oxidation of H2, and the role of chemisorbed H. Electrochim. Acta 47, 3571–3594. http://dx.doi.org/10.1016/S0013-4686(02)00329-8.

Conway, B.E.B., Salomon, M., 1964. Electrochemical reaction orders: applications to the hydrogen- and oxygen-evolution reactions. Electrochim. Acta 9, 1599–1615. http://dx.doi.org/10.1016/0013-4686(64)80088-8.

Crolet, J.-L., Thevenot, N., Dugstad, A., 1999. Role of free acetic acid on the CO_2 corrosion of steels. In: Corrosion 1999. Paper No. 24.

Cussler, E.L., 1997. Diffusion: Mass Transfer in Fluid Systems, Cambridge Series in Chemical Engineering. Cambridge University Press.

Davies, D.H., Burstein, T., 1980. The effect of bicarbonate on the corrosion and passivation of iron. Corrosion 36, 416–422.

Davies, J.T., 1972. Turbulence phenomena.

Dayalan, E., de Moraes, F.D., Shadley, J.R., Shirazi, S. a, Rybicki, E.F., 1998. CO_2 corrosion Prediction in Pipe Flow under $FeCO_3$ Scale-forming Conditions. Nace International. Paper No. 51.

Dayalan, E., Vani, G., Shadley, J.R., Shirazi, S.A., Rybicki, E.F., 1995. Modeling CO_2 Corrosion of Carbon Steels in Pipe Flow. Nace International. Paper No. 118.

De Waard, C., Lotz, U., 1993. Prediction of CO_2 Corrosion of Carbon Steel. Nace International. Paper No. 069.

De Waard, C., Lotz, U., Dugstad, A., 1995. Influence of Liquid Flow Velocity on CO2 Corrosion: a Semi-empirical Model. Nace International. Paper No. 128.

De Waard, C., Lotz, U., Milliams, D.E., 1991. Predictive model for CO_2 corrosion engineering in wet natural gas pipelines. Corrosion 47, 976–985. http://dx.doi.org/

10.5006/1.3585212.
De Waard, C., Milliams, D.E., 1975a. Carbonic acid corrosion of steel. Corrosion 31, 177–181. http://dx.doi.org/10.5006/0010-9312-31.5.177.
De Waard, C., Milliams, D.E., 1975b. Prediction of carbonic acid corrosion in natural gas pipelines. In: Internal and External Protection of Pipes. F1-1-F1-8.
Delahay, P. (Ed.), 1970. Advances in Electrochemistry and Electrochemical Engineering. Electrochemistry, Advances in Electrochemistry and Electrochemical Engineering, vol. 7. Interscience.
Delahay, P., 1952. Implications of the kinetics of ionic dissociation with regard to some electrochemical processes—application to polarography. J. Am. Chem. Soc. 74, 3497–3500. http://dx.doi.org/10.1021/ja01134a013.
Dickson, A.G., Goyet, C. (Eds.), 1994. DOE Handbook of Methods for the Analysis of the Various Parameters of the Carbon Dioxide System in Sea Water, second ed.
Duan, Z., Li, D., 2008. Coupled phase and aqueous species equilibrium of the H_2O–CO_2–NaCl–CaCO3 system from 0 to 250°C, 1 to 1000bar with NaCl concentrations up to saturation of halite. Geochim. Cosmochim. Acta 72, 5128–5145. http://dx.doi.org/10.1016/j.gca.2008.07.025.
Duan, Z., Sun, R., 2003. An improved model calculating CO_2 solubility in pure water and aqueous NaCl solutions from 273 to 5333 K and from 0 to 2000 bar. Chem. Geol. 193, 257–271. http://dx.doi.org/10.1016/s0009-2541(02)00263-2.
Duan, Z., Sun, R., Zhu, C., Chou, I.-M., 2006. An improved model for the calculation of CO_2 solubility in aqueous solutions containing Na+, K+, Ca2+, Mg2+, Cl−, and SO_4^{2-}. Mar. Chem. 98, 131–139. http://dx.doi.org/10.1016/j.marchem.2005.09.001.
Dugstad, A., 1998. Mechanism of Protective Film Formation during CO_2 Corrosion of Carbon Steel. Nace International. Paper No. 31.
Dugstad, A., Lunde, L., Videm, K., 1994. Parametric Study of CO_2 Corrosion of Carbon Steel. Nace International. Paper No. 14.
Fajardo, V., Canto, C., Brown, B., Nešić, S., 2007. Effects of Organic Acids in CO_2 Corrosion. Nace International. Paper No. 319.
Farelas, F., Choi, Y.-S., Nešić, S., Magalhães, A.A.O., de Azevedo Andrade, C., 2014. Corrosion behavior of deep water oil production tubing material under supercritical CO_2 environment: part 2—effect of crude oil and flow. Corrosion 70, 137–145. http://dx.doi.org/10.5006/1019.
Farelas, F., Galicia, M., Brown, B., Nesic, S., Castaneda, H., 2010. Evolution of dissolution processes at the interface of carbon steel corroding in a CO_2 environment studied by EIS. Corros. Sci. 52, 509–517. http://dx.doi.org/10.1016/j.corsci.2009.10.007.
Felloni, L., 1968. The effect of pH on the electrochemical behaviour of iron in hydrochloric acid. Corros. Sci. 8, 133–148. http://dx.doi.org/10.1016/S0010-938X(68)80196-9.
Fosbøl, P.L., Thomsen, K., Stenby, E.H., 2009. Improving Mechanistic CO_2 Corrosion Models. Nace International. Paper No.561.
Garsany, Y., Pletcher, D., Hedges, B., 2002. The Role of Acetate in CO_2 Corrosion of Carbon Steel: Has the Chemistry Been Forgotten? Nace International. Paper No. 273.
Gennero de Chialvo, M.R., Chialvo, A.C., 2001. Hydrogen evolution reaction on a smooth iron electrode in alkaline solution at different temperatures. Phys. Chem. Chem. Phys. 3, 3180–3184. http://dx.doi.org/10.1039/b102777h.
Gennero de Chialvo, M.R., Chialvo, A.C., 2000. Existence of two sets of kinetic parameters in the correlation of the hydrogen electrode reaction. J. Electrochem. Soc. 147, 1619–1622.
Gennero de Chialvo, M.R., Chialvo, A.C., 1999. The Tafel-Heyrovsky route in the kinetic mechanism of the hydrogen evolution reaction. Electrochem. Commun 1, 379–382. http://dx.doi.org/10.1016/s1388-2481(99)00078-8.
Gennero de Chialvo, M.R., Chialvo, A.C., 1998. Kinetics of hydrogen evolution reaction with frumkin adsorption: re-examination of the Volmer-Heyrovsky and Volmer-Tafel routes. Electrochim. Acta 44, 841–851. http://dx.doi.org/10.1016/S0013-4686(98)00233-3.
George, K., Nešić, S., de Waard, C., 2004. Electrochemical Investigation and Modeling of Carbon Dioxide Corrosion of Carbon Steel in the Presence of Acetic Acid. Nace International. Paper No. 379.
George, K.S., Nešic, S., 2007. Investigation of carbon dioxide corrosion of mild steel in the presence of acetic acid-part 1: basic mechanisms. Corrosion 178–186. http://dx.doi.org/10.5006/1.3278342.
Gray, L.G.S., Anderson, B.G., Danysh, M.J., Tremaine, P.R., 1990. Effect of pH and Temperature on the Mechanism of Carbon Steel Corrosion by Aqueous Carbon Dioxide. Nace International. Paper No. 40.
Gray, L.G.S., Anderson, B.G., Danysh, M.J., Tremaine, P.R., 1989. Mechanisms of Carbon Steel Corrosion in Brines Containing Dissolved Carbon Dioxide at Ph 4. Nace International. Paper No. 464.
Green, N. (Ed.), 1972. Comprehensive Chemical Kinetics, vol. 6. Elsevier Inc, Amsterdam, The Netherlands.
Gulbrandsen, E., 2007. Acetic Acid and Carbon Dioxide Corrosion of Carbon Steel Covered with Iron Carbonate. Nace International. Paper No. 322.
Gulbrandsen, E., Bilkova, K., 2006. Solution Chemistry Effects on Corrosion of Carbon Steels in Presence of CO_2 and Acetic Acid. Nace International. Paper No. 06364.
Han, J., Carey, J.W., Zhang, J., 2011a. A coupled electrochemical-geochemical model of corrosion for mild steel in high-pressure CO_2-saline environments. Int. J. Greenh. Gas. Control 5, 777–787. http://dx.doi.org/10.1016/j.ijggc.2011.02.005.
Han, J., Carey, J.W., Zhang, J., 2011b. Effect of sodium chloride on corrosion of mild steel in CO_2-saturated brines. J. Appl. Electrochem 41, 741–749. http://dx.doi.org/10.1007/s10800-011-0290-3.
Han, J., Zhang, J., Carey, J.W., 2011c. Effect of bicarbonate on corrosion of carbon steel in CO_2 saturated brines. Int. J. Greenh. Gas. Control 5, 1680–1683. http://dx.doi.org/10.1016/j.ijggc.2011.08.003.
Hurlen, T., 1960. Electrochemical behaviour of iron. Acta Chem. Scand. 14, 1533–1554. http://dx.doi.org/10.3891/acta.chem.scand.14-1533.
Hurlen, T., Gunvaldsen, S., Blaker, F., 1984. Effects of buffers on hydrogen evolution at iron electrodes. Electrochim. Acta 29, 1163–1164. http://dx.doi.org/10.1016/0013-4686(84)87171-6.
Jangama, V.R., Srinivasan, S., 1997. A Computer Model for Prediction of Corrosion of Carbon Steels. Nace International. Paper No. 318.
Johnson, M.L., Tomson, M.B., 1991. Ferrous carbonate precipitation kinetics and its impact on CO_2 corrosion. Nace Int. Paper No. 268.
Joosten, M., Owens, D., Hobbins, A., Sun, H., Achour, M., Lanktree, D., 2010. Top-of-Line Corrosion – a Field Failure. EuroCorr. Paper No. 9524.
Juodkazis, K., Juodkazyt, J., Grigucevičien, A., Juodkazis, S., 2011. Hydrogen species within the metals: role of molecular hydrogen ion H2+. Appl. Surf. Sci. 258, 743–747. http://dx.doi.org/10.1016/j.apsusc.2011.08.054.
Juodkazis, K., Juodkazyte, J., Šebeka, B., Juodkazis, S., 2014. Reversible hydrogen evolution and oxidation on Pt electrode mediated by molecular ion. Appl. Surf. Sci. 290, 13–17. http://dx.doi.org/10.1016/j.apsusc.2013.10.164.
Kapusta, S.D., Pots, B.F.M., Rippon, I.J., 2004. The Application of Corrosion Prediction Models to the Design and Operation of Pipelines. Nace International.
Kermani, M.B., Morshed, A., 2003. Carbon dioxide corrosion in oil and gas production – a compendium. Corrosion 59, 659–683. http://dx.doi.org/10.5006/1.3277596.
Kittel, J., Ropital, F., Grosjean, F., Sutter, E.M.M., Tribollet, B., 2013. Corrosion mechanisms in aqueous solutions containing dissolved H_2S. Part 1: Characterisation of H_2S reduction on a 316L rotating disc electrode. Corros. Sci. 66, 324–329. http://dx.doi.org/10.1016/j.corsci.2012.09.036.
Lasaga, A.C., 1998. Kinetic Theory in the Earth Sciences. Princeton University Press.
Li, D., Duan, Z., 2007. The speciation equilibrium coupling with phase equilibrium in the H2O–CO_2–NaCl system from 0 to 250 °C, from 0 to 1000 bar, and from 0 to 5 molality of NaCl. Chem. Geol. 244, 730–751. http://dx.doi.org/10.1016/j.chemgeo.2007.07.023.
Matos, M., Canhoto, C., Bento, M.F., Geraldo, M.D., 2010. Simultaneous evaluation of the dissociated and undissociated acid concentrations by square wave voltammetry using microelectrodes. J. Electroanal. Chem. 647, 144–149. http://dx.doi.org/10.1016/j.jelechem.2010.06.010.
McCafferty, E., Hackerman, N., 1972. Kinetics of iron corrosion in concentrated acid chloride solutions. J. Electrochem. Soc. 119, 999–1009.
Menaul, P., 1944. Causative agents of corrosion in distillate field. Oil Gas. J. 43, 80–81.
Millero, F.J., 1995. Thermodynamics of the carbon dioxide system in the oceans. Geochim. Cosmochim. Acta 59, 661–677. http://dx.doi.org/10.1016/0016-7037(94)00354-O.
Mishra, B., Al-Hassan, S., Olson, D.L., Salama, M.M., 1997. Development of a predictive model for activation-controlled corrosion of steel in solutions containing carbon dioxide. Corrosion 53, 852–859. http://dx.doi.org/10.5006/1.3290270.
Mohamed, M.F., Nor, A.M., Suhor, M.F., Singer, M., Choi, Y.S., Technology, M., 2011. Water chemistry for corrosion prediction in high pressure CO_2 environments. Nace International. Paper No. 375.
Nešić, S., 2011. Carbon Dioxide Corrosion of Mild Steel, third ed. In: Uhlig's Corrosion Handbook, pp. 229–245. http://dx.doi.org/10.1002/9780470872864.ch19
Nešić, S., 2007. Key issues related to modelling of internal corrosion of oil and gas pipelines – a review. Corros. Sci. http://dx.doi.org/10.1016/j.corsci.2007.06.006.
Nešić, S., Lee, J., Ruzic, V., 2002. A Mechanistic Model of Iron Carbonate Film Growth and the Effect on CO_2 Corrosion of Mild Steel. Nace International. Paper No. 237.
Nešić, S., Lee, K.L.J., 2003. A mechanistic model for carbon dioxide corrosion of mild steel in the presence of protective iron carbonate films – part 3: film growth model. Corrosion 59, 616–628. http://dx.doi.org/10.5006/1.3277592.
Nešić, S., Li, H., Huang, J., Sormaz, D., 2009. An Open Source Mechanistic Model for CO_2/H_2S Corrosion of Carbon Steel. Nace International. Paper No. 09572.
Nešić, S., Nordsveen, M., Nyborg, R., Stangeland, A., 2003. A mechanistic model for carbon dioxide corrosion of mild steel in the presence of protective iron carbonate films—Part 2: a numerical experiment. Corrosion 59, 489–497. http://dx.doi.org/10.5006/1.3277592.
Nešić, S., Nordsveen, M., Nyborg, R., Stangeland, A., 2001. A Mechanistic Model for Co_2 Corrosion With Protective Iron Carbonate Films. Nace International. Paper No. 040.
Nešić, S., Postlethwaite, J., Olsen, S., 1996a. An electrochemical model for prediction of corrosion of mild steel in aqueous carbon dioxide solutions. Corrosion 52, 280–294.
Nešić, S., Postlethwaite, J., Thevenot, N., 1995. Superposition of diffusion and chemical reaction controlled limiting current -application to CO_2 corrosion. J. Corros. Sci. Eng. 1, 1–14.
Nešić, S., Postlethwaite, J., Vrhovac, M., 1997. CO_2 corrosion of carbon steel – from mechanistic to empirical modelling. Corros. Rev. 15, 211–240.
Nešić, S., Sun, W., 2010. Corrosion in Acid Gas Solutions. Shreir's Corrosion, pp. 1270–1298.
Nešić, S., Thevenot, N., Crolet, J.L., Drazic, D., 1996b. Electrochemical Properties of Iron Dissolution in the Presence of CO_2 – Basics Revisited. Nace International. Paper No. 03.
Newman, J., Thomas-Alyea, K.E., 2004. Electrochemical Systems, third ed. Wiley-interscience.

Newman, J.S., 1973. Electrochemical Systems, first ed. Prentice Hall, Inc.
Nordsveen, M., Nešić, S., Nyborg, R., Stangeland, A., 2003. A mechanistic model for carbon dioxide corrosion of mild steel in the presence of protective iron carbonate films – part 1: theory and verification. Corrosion 59, 443–456. http://dx.doi.org/10.5006/1.3277592.
Nyborg, R., 2006. Field data Collection, evaluation and use for Corrosivity prediction and validation of models. Nace International. Paper no. 118.
Nyborg, R., 2002. Overview of CO_2 Corrosion Models For Models for Wells And Pipelines. Nace International. Paper No. 233.
Nyborg, R., Andersson, P., Nordsveen, M., 2000. Implementation of CO_2 Corrosion Models in a Three-Phase Fluid Flow Model. Nace International. Paper No. 048.
Nyborg, R., Dugstad, A., 2007. Top of Line Corrosion and Water Condensation Rates in Wet Gas Pipelines. Nace International. Paper No. 555.
Ogundele, G.I., White, W.E., 1987. Observations on the influences of dissolved hydrocarbon gases and variable water Chemistries on corrosion of an Api-L80 steel. Corrosion 43, 665–673. http://dx.doi.org/10.5006/1.3583847.
Ogundele, G.I., White, W.E., 1986. Some observations on corrosion of carbon steel in aqueous environments containing carbon dioxide. Corrosion 42, 71–78. http://dx.doi.org/10.5006/1.3584888.
Okafor, P.C., Brown, B., Nešić, S., 2009. CO_2 corrosion of carbon steel in the presence of acetic acid at higher temperatures. J. Appl. Electrochem 39, 873–877. http://dx.doi.org/10.1007/s10800-008-9733-x.
Olsen, S., 2003. CO_2 Corrosion Prediction by Use of the Norsok M-506 Model – Guidelines and Limitations. Nace International. Paper No. 623.
Olsen, S., Halvorsen, A.M., Lunde, Per G., Nyborg, R., 2005. CO_2 Corrosion Prediction Model – Basic Principles. Nace International. Paper No. 551.
Paillassa, R., Dieumegard, M., Estavoyer, M.M., 1963. Corrosion control in the gathering system at LACQ sour Gas field. In: 2nd Intl. Congress on Metallic Corrosion, pp. 410–417.
Palmer, D. a., Eldik, R. Van, 1983. The chemistry of metal carbonat and carbon dioxide complexes. Chem. Rev. 83, 651–731. http://dx.doi.org/10.1021/cr00058a004.
Pentland, N., Bockris, J.O., Sheldon, E., 1957. Hydrogen evolution reaction on Copper, gold, molybdenum, Palladium, rhodium, and iron. J. Electrochem. Soc. 104, 182. http://dx.doi.org/10.1149/1.2428530.
Pfennig, a., Bäßler, R., 2009. Effect of CO_2 on the stability of steels with 1% and 13% Cr in saline water. Corros. Sci. 51, 931–940. http://dx.doi.org/10.1016/j.corsci.2009.01.025.
Pfennig, A., Kranzmann, A., 2011. Reliability of pipe steels with different amounts of C and Cr during onshore carbon dioxide injection. Int. J. Greenh. Gas. Control 5, 757–769. http://dx.doi.org/10.1016/j.ijggc.2011.03.006.
Pfennig, A., Kranzmann, A., 2009. Effect of CO_2 and pressure on the stability of steels with different amounts of chromium in saline water. Corros. Sci. 51, 931–940.
Pots, B.F.M., 1995. Mechanistic Models for the Prediction of CO_2 Corrosion Rates under Multi-Phase Flow Conditions. Nace International. Paper No. 137.
Pots, B.F.M., Hendriksen, E.L.J. a, 2000. CO_2 Corrosion Under Scaling Conditions – The Special Case of Top-of-Line Corrosion in Wet Gas Pipelines. Nace International. Paper No. 031.
Pots, B.F.M., John, R.C., Rippon, I.J., Thomas, M.J.J.S., Kapusta, S.D., Grigs, M.M., Whitham, T., 2002. Improvements on de Waard-Milliams Corrosion Prediction and Applications to Corrosion Management. Nace International. Paper No. 235.
Poulson, B., 1991. Measuring and modelling mass transfer at bends in annular two phase flow. Chem. Eng. Sci. 46, 1069–1082. http://dx.doi.org/10.1016/0009-2509(91)85100-C.
Qian, S.Y., Conway, B.E., Jerkiewicz, G., 1999. Electrochemical sorption of H into Fe and mild-steel: kinetic conditions for enhancement or inhibition by adsorbed HS. Phys. Chem. Chem. Phys. 1, 2805–2813. http://dx.doi.org/10.1039/a901369e.
Qian, S.Y., Conway, B.E., Jerkiewicz, G., 1998. Kinetic rationalization of catalyst poison effects on cathodic H sorption into metals: relation of enhancement and inhibition to H coverage. J. Chem. Soc. Faraday Trans. 94, 2945–2954. http://dx.doi.org/10.1039/a804113j.
Rajappa, S., Zhang, R., Gopal, M., 1998. Modeling the Diffusion Effects through the Iron Carbonate Layer in the Carbon Dioxide Corrosion of Carbon Steel. Nace International. Paper No. 026.
Remita, E., Tribollet, B., Sutter, E., Vivier, V., Ropital, F., Kittel, J., 2008. Hydrogen evolution in aqueous solutions containing dissolved CO_2: quantitative contribution of the buffering effect. Corros. Sci. 50, 1433–1440. http://dx.doi.org/10.1016/j.corsci.2007.12.007.
Revie, R.W. (Ed.), 2011. Uhlig's Corrosion Handbook, first ed. John Wiley & Sons, Inc., Hoboken, NJ, USA.
Richardson, T. (Ed.), 2009. Shreir's Corrosion, first ed. Elsevier Science.
Roy, R.N., Roy, L.N., Vogel, K.M., Porter-Moore, C., Pearson, T., Good, C.E., Millero, F.J., Campbell, D.M., 1993. The dissociation constants of carbonic acid in seawater at salinities 5 to 45 and temperatures 0 to 45°C. Mar. Chem. 44, 249–267. http://dx.doi.org/10.1016/0304-4203(93)90207-5.
Ruhl, A.S., Kranzmann, A., 2013. Investigation of corrosive effects of sulphur dioxide, oxygen and water vapour on pipeline steels. Int. J. Greenh. Gas. Control 13, 9–16. http://dx.doi.org/10.1016/j.ijggc.2012.12.007.
Ruhl, A.S., Kranzmann, A., 2012. Corrosion behavior of various steels in a continuous flow of carbon dioxide containing impurities. Int. J. Greenh. Gas. Control 9, 85–90. http://dx.doi.org/10.1016/j.ijggc.2012.03.005.
Ruzic, V., Veidt, M., Nešić, S., 2007. Protective iron carbonate films—part 3: simultaneous chemo-mechanical removal in single-phase aqueous flow. Corrosion 63, 758–769. http://dx.doi.org/10.5006/1.3278425.
Ruzic, V., Veidt, M., Nešsić, S., 2006a. Protective iron carbonate films—part 2: chemical removal by dissolution in single-phase aqueous flow. Corrosion 62, 598–611. http://dx.doi.org/10.5006/1.3280674.
Ruzic, V., Veidt, M., Nešsić, S., 2006b. Protective iron carbonate films—part 1: mechanical removal in single-phase aqueous flow. Corrosion 62, 419–432.
Safizadeh, F., Ghali, E., Houlachi, G., 2015. Electrocatalysis developments for hydrogen evolution reaction in alkaline solutions – a review. Int. J. Hydrogen Energy 40, 256–274. http://dx.doi.org/10.1016/j.ijhydene.2014.10.109.
Schmitt, G., Rothmann, B., 1977. Studies on the corrosion mechanism of unalloyed steel in oxygen-free carbon dioxide solutions part I. kinetics of the liberation of hydrogen. Werkst. Korros. 28, 816.
Schuldiner, S., 1961. Kinetics of hydrogen evolution at zero hydrogen partial pressure. J. Electrochem. Soc. 108, 384. http://dx.doi.org/10.1149/1.2428093.
Schuldiner, S., 1954a. Hydrogen overvohage on bright platinunl II. pH and salt effects in acid, neutral, and alkaline solutions. J. Electrochem. Soc. 101, 426–432.
Schuldiner, S., 1954b. Hydrogen overvoltage on bright platinum. J. Electrochem. Soc. 101, 426. http://dx.doi.org/10.1149/1.2781294.
Sheng, W., Gasteiger, H.A., Shao-Horn, Y., 2010. Hydrogen oxidation and evolution reaction kinetics on platinum: acid vs alkaline electrolytes. J. Electrochem. Soc. 157, B1529–B1536. http://dx.doi.org/10.1149/1.3483106.
Singer, M., 2013. Study and Modeling of the Localized Nature of Top of the Line Corrosion. PhD Diss. Ohio University.
Singer, M., Hinkson, D., Zhang, Z., Wang, H., Nes, S., 2013. CO_2 top-of-the-line corrosion in presence of acetic acid: a Parametric study. Corrosion 69, 719–735.
Song, F.M., 2010. A comprehensive model for predicting CO_2 corrosion rate in oil and gas production and transportation systems. Electrochim. Acta 55, 689–700. http://dx.doi.org/10.1016/j.electacta.2009.07.087.
Song, F.M., Kirk, D.W., Graydon, J.W., Cormack, D.E., 2004. Predicting carbon dioxide corrosion of bare steel under an aqueous boundary layer. Corrosion 60, 736–748. http://dx.doi.org/10.5006/1.3287866.
Stern, M., 1955. The electrochemical behavior, including hydrogen overvoltage, of iron in acid environments. J. Electrochem. Soc. 102, 609–616.
Stumm, W., Morgan, J.J., 1995. Aquatic Chemistry: Chemical Equilibria and Rates in Natural Waters.
Sun, W., Nesic, S., 2006. Basics Revisited: Kinetics of Iron Carbonate Scale Precipitation in CO_2 Corrosion. Nace International. Paper No. 365.
Sun, W., Nešić, S., 2008. Kinetics of corrosion layer formation: part 1 – iron carbonate layers in carbon dioxide corrosion. Corrosion 64, 334–346. http://dx.doi.org/10.5006/1.3278494.
Sun, W., Nešić, S., Woollam, R.C., 2009. The effect of temperature and ionic strength on iron carbonate ($FeCO_3$) solubility limit. Corros. Sci. 51, 1273–1276. http://dx.doi.org/10.1016/j.corsci.2009.03.009.
Sun, Y., George, K., Nešić, S., 2003. The Effect of Cl- and Acetic Acid on Localized CO_2 Corrosion in Wet Gas Flow. Nace International. Paper No. 327.
Sundaram, M., Raman, V., High, M.S., Tree, D. a, Wagner, J., 1996. Deterministic Modeling of Corrosion in Downhole Environments. Nace International. Paper No. 30.
Tavares, M.C., Machado, S.A.S., Mazo, L.H., 2001. Study of hydrogen evolution reaction in acid medium on Pt microelectrodes. Electrochim. Acta 46, 4359–4369. http://dx.doi.org/10.1016/S0013-4686(01)00726-5.
Thomas, N.T., Nobe, K., 1970. Kinetics of the hydrogen evolution reaction on titanium. J. Electrochem. Soc. 117, 622. http://dx.doi.org/10.1149/1.2407590.
Tilak, B.V., Chen, C.P., 1993. Generalized analytical expressions for Tafel slope, reaction order and a.c. impedance for the hydrogen evolution reaction (HER): mechanism of HER on platinum in alkaline media. J. Appl. Electrochem 23, 631–640. http://dx.doi.org/10.1007/BF00721955.
Tran, T., Brown, B., Nešić, S., 2015. Corrosion of Mild Steel in an Aqueous CO_2 Environment – Basic Electrochemical Mechanisms Revisited. Nace International. Paper no. 671.
Tran, T., Brown, B., Nešic, S., Tribollet, B., 2013. Investigation of the electrochemical mechanisms for acetic acid corrosion of mild steel. Corrosion 70, 223–229.
Tribollet, B., Kittel, J., Meroufel, A., Ropital, F., Grosjean, F., Sutter, E.M.M., 2014. Corrosion mechanisms in aqueous solutions containing dissolved H_2S. Part 2: model of the cathodic reactions on a 316L stainless steel rotating disc electrode. Electrochim. Acta 124, 46–51. http://dx.doi.org/10.1016/j.corsci.2012.09.036.
Turgoose, S., Cottis, R.A., Lawson, K., 1992. Modeling of electrode processes and surface chemistry in carbon dioxide containing solutions, in: Computer modeling in Corrosion. ASTM STP 1154, 67–81.
Van Hunnik, E.W.J., Pots, B.F.M., Hendriksen, E.L.J. a, 1996. The Formation of Protective $FeCO_3$ Corrosion Product Layers in CO_2 Corrosion. Nace International. Paper No. 006.
Videm, K., 1993. Fundamental studies aimed at improving models for prediction of CO_2 corrosion of carbon steels. In: Progress in the Understanding and Prevention of Corrosion, p. 507.
Wang, J., Shirazi, S. a, 2001. A CFD based correlation for mass transfer coefficient in elbows. Int. J. Heat. Mass Transf. 44, 1817–1822.
Wang, J., Shirazi, S. a, Shadley, J.R., Rybicki, E.F., Dayalan, E., 1998. A Correlation for Mass Transfer Coefficients in Elbows. Nace International. Paper no. 42.
Weiss, R.F., 1974. Carbon dioxide in water and sea water: the solubility of a non-ideal gas. Mar. Chem. 2, 203–215.
Więckowski, A., Ghali, E., Szklarczyk, M., Sobkowski, J., 1983a. The behaviour of iron electrode in CO_2– saturated neutral electrolyte—I. Electrochemical study. Electrochim. Acta 28, 1619–1626.
Więckowski, A., Ghali, E., Szklarczyk, M., Sobkowski, J., 1983b. The behaviour of iron electrode in CO_2– saturated neutral electrolyte—II. Radiotracer study and

corrosion considerations. Electrochim. Acta. http://dx.doi.org/10.1016/0013-4686(83)85227-X.
Zeebe, R.E., Wolf-Gladrow, D. (Eds.), 2001. CO_2 in Seawater: Equilibrium, Kinetics, Isotopes. Elsevier Oceanography Series, Elsevier. http://dx.doi.org/10.1016/S0422-9894(01)80001-5.
Zhang, Z., Hinkson, D., Singer, M., Wang, H., Nešić, S., 2007. A mechanistic model of top-of-the-line corrosion. Corrosion 63, 1051–1062. http://dx.doi.org/10.5006/1.3278321.
Zheng, Y., Brown, B., Nešic, S., 2014. Electrochemical study and modeling of H_2S corrosion of mild steel. Corrosion 70, 351–365.